INFN-PI-AE-93-02
Fermilab Library
0 1160 0023666 5

January 11, 1993
INFN-PI/AE-93/02

GRAVITATIONAL WAVE DETECTION BY MICHELSON INTERFEROMETRY

R.Del Fabbro
I.N.F.N. Sezione di Pisa, Pisa, Italy

V.Montelatici[1]
E.N.E.A., Laboratori di Frascati,Roma, Italy

Abstract

Michelson interferometry devoted to gravitational wave detection is reviewed in the most important achievements reached in the last decade.
The matter of the interferometric antenna theory has been studied in the framework of the antenna reference system (FNC system); results agree with these ones available in the literature obtained in the framework of the transfer traceless reference system (TT system).

[1] On leave of absence from ENEA, Frascati (Roma); present address INFN Section of Pisa

January 11, 1993
INFN PI/AE 93/01

GRAVITATIONAL WAVE DETECTION BY MICHELSON INTERFEROMETRY

R.Del Fabbro
I.N.F.N. Sezione di Pisa, Pisa, Italy

V.Montelatici[1]
E.N.E.A., Laboratori di Frascati,Roma, Italy

Abstract

Michelson interferometry devoted to gravitational wave detection is reviewed in the most important achievements reached in the last decade.
The matter of the interferometric antenna theory has been studied in the framework of the antenna reference system (FNC system); results agree with these ones available in the literature obtained in the framework of the transfer traceless reference system (TT system).

[1]On leave of absence from ENEA, Frascati (Roma); present address INFN Section of Pisa

1.Introduction

One of the most exciting research field is undoubtly that one devoted to attain the direct observation[1,2] of gravitational waves (GW) emitted by cosmic sources.
Since the Foward's paper[3] (1979) till nowadays remarkable progresses and developments have been done in Michelson interferometry in order to gain more and more sensitivity in GW detectors.
Let us review the most important achievements of this last ten years, like the equipment of the Michelson arms with delay lines[4] or resonant Fabry-Perot (FP) cavities[5] in order to enlarge optically the interferometer armlength; the recycling technique[6] saving the reflected light in order to have more power at disposal and therefore more sensitivity; the proposed "dual mode" technique[7], which introduces a recycling mirror in the transmission branch of the intereferometer in order to get a better stability and less criticity to noise.
In addition it has been shown that the interferometer can be used[8] either as a wide band detector or it can be tuned in order to get a larger sensitivity in a narrow frequency band.
Besides these technical improvements a noticeable theoretical work[8,9,10] has been done on the interaction of GW with the e.m. field inside an interferometric antenna.
These studies have produced predictions of the intereferometric antenna sensitivities in different configurations (delay lines, F.P. cavities, recycling, synchronous mode, dual mode etc).
Furthermore studies[5,11,12,21] have been performed on the misalignment effects of the interferometer optical elements and their functional behaviour as noise sources.
All these scientific achievements are fundamental milestones for the projects[5,11] nowadays in progress of grounded base kilometric scale interferometers.
In this paper it is our aim to review the matter and to discuss the most remarkable problems concerning the GW interferometry.
In section 2 the Michelson interferometry is introduced and the S-matrix technique is briefly described.
In section 3 the theory of the interferometric antennas equipped with FP cavities in the Michelson arms and recycling technique is discussed, giving

the field expressions and the associated resonance conditions.
In section 4 the previous section achievements are applied to the VIRGO project case.
In section 5 the antenna sensitivity is discussed in the case of broad band configuration of the interferometer.
In section 6 the antenna sensitivity is presented in the case of narrow band optical version.
In section 7 a brief discussion is given on the validity limits of results achieved in the previous sections.
Finally four appendices are added in order to supply the possibility to go deeper in the matter and,in some cases, to facilitate the deduction of formulas given in the text.
It is worth while to remark that the given results, involving the effect of the gravitational field, have been obtained working in the *Fermi Normal Coordinates* (FNC) reference system [1].
In fact, if the interaction of the gravitational field with the e.m. field is considered, it is very important the reference system chosen in describing the interaction.
Two important frames are a possible choice: the transvers traceless (TT) reference frame travelling with the gravitational wave and the FNC frame at rest with the interferometer.
In the TT reference system the optical elements of the interferometer are *seen* fixed and the gravitational-electromagnetic interaction produces a time phase shift corresponding to the delay time in a *round trip* of the light travelling into the intereferometer arms.
The interaction between the gravitational and e.m. field is just the perturbed invariant $(ds)^2$, that in the TT frame is written :

$$(ds)^2 = c^2 (dt)^2 - dx^2 (1 + h(t)) - dy^2 (1 - h(t)) = 0 \tag{1}$$

where $h(t) = h \cos(\Omega t)$ and the GW, polarized along the interferometer arms, travels in the normal direction of the interferometer plane.
It results that the total phase shift $\Phi_{TT}(t)$ registered by the interferometer

[1] Note that so far in the literature (see refs.8,9) the gravitational-e.m. field interaction has been studied in the TT reference system.

of armlength d_0 at first order in h ($h << 1$) is :

$$\Phi_{TT}(t) = \omega(\Delta t_x - \Delta t_y) = hk2d_0 \frac{\sin(d_0\Omega/c)}{d_0\Omega/c} \cos(\Omega t - \Omega d_0/c) \tag{2}$$

The (2) shows that the effect of the gravitational wave on the interferometer is just a delay time of the light path along the interferometer arms.
On the other hand, as shown by Fortini and Ortolan[10], in the FNC frame the crossing of a GW gives a phase shift as sum of two components: the interaction with the e.m. field producing a time phase shift $\Phi_{\Delta t}$ and the space deformation producing a space phase shift $\Phi_{\Delta s}$.
In fact in the FNC reference system the optical elements of the interferometer are no longer *at rest*, because they *feel* the ripple of the space curvature produced by the GW crossing. The space and time phases are:

$$\begin{aligned} \Phi_{\Delta s} &= hk2d_0 \cos(\Omega t - \Omega d_0/c) \\ \Phi_{\Delta t} &= hk2d_0 \cos(\Omega t - \Omega d_0/c) \left(1 - \frac{\sin(\Omega d_0/c)}{\Omega d_0/c}\right) \end{aligned} \tag{3}$$

and the total phase shift $\Phi_{FNC}(t)$ is :

$$\Phi_{FNC}(t) = \Phi_{\Delta s} - \Phi_{\Delta t} = hk2d_0 \frac{\sin(\Omega d_0/c)}{\Omega d_0/c} \cos(\Omega t - \Omega d_0/c) \tag{4}$$

the expression (4) turns out to be equal to expression (2) according to the gauge invariance character of the total phase shift.
As stressed by Fortini and Ortolan[13], the gravitational phase shift measured by an interferometric antenna is a combined effect of both space and time phases. However in the FNC reference system, also for kilometric arm interferometers, the time phase is negligible with respect to the spatial one (as it is apparent by the expression (3)) as long as the interferometer armlength d_0 is much smaller than the gravitational wave armlength λ_g ($\Omega d_0/c = 2\pi d_0/\lambda_g \sim 10^{-2}$).
That is the reason why in the calculations it has been put $\mathrm{sinc}(\Omega d_0/c) \simeq 1$ throughout this paper.

2.Michelson interferometry and S-matrix

The Michelson interferometer[14,15], by splitting an incoming laser beam in two symmetric propagating fields, is an optical device, which supplies two interfering output beams : the reflected beam directed toward the source and the transmitted beam directed transversally to the source direction (see Fig.1a).
The interference characters of the output beams (constructive or destructive interference) are complementary for evident energy flux conservation.
It is well known that the Michelson interferometer can detect very small optical length difference between the two interferometer arms by observing the intensity variations in the transmitted beam. It can be shown that the best sensitivity is obtained in the condition of destructive interference (the so called dark fringe operating point). Therefore in the standard conditions almost the total laser intensity is reflected backward.
Since the interferometer sensitivity is proportional to the square root of the laser power, it is in general convenient to use the reflected intensity by adding a reflecting mirror capable to recycling the power back again toward the interferometer (see Fig. 1b).
This technique[6] increases the power circulating into the interferometer as if fed by a larger power laser by the so called recycling factor.
Going on in the quantitative discussion of the Michelson inteferometry,the technical tools and the relative notations will be given.
The Michelson interferometer is built up by optical elements capable of reflecting and transmitting the light and therefore characterized by a reflectivity R and a transmittivity T defined as follows :

$$R = r^2 \qquad T = t^2 \tag{1}$$

where r is the reflectance and t the transmittance of the optical element.
The energy conservation requires the fulfillment of the relation :

$$R + T = \sigma = 1 - \varepsilon^2 \tag{2}$$

where ε^2 is the term describing the energy-losses into the optical element.
A typical reflecting optical element is constituted by a glass having a portion of its surface coated by rare-earth oxide. The thickness of this coated

layer and in general its deposition technique, as the multi-layers interferential coating, fixes the parameters r, t and ε for a given light beam wavelength . By the S-matrix technique[16] the fields reflected and transmitted by an optical element can be calculated taking into account properly the external and internal reflection phase change:

$$\begin{vmatrix} A_R \\ A_T \end{vmatrix} = \begin{vmatrix} t & ir \\ ir & t \end{vmatrix} \begin{vmatrix} A' \\ A_{IN} \end{vmatrix} \qquad S - matrix = \begin{vmatrix} t & ir \\ ir & t \end{vmatrix} \tag{3}$$

where A_{IN}, A_T and A_R indicate the incoming, the transmitted and the reflected fields and A' is a back incoming field (see Fig. 1d).
In addition a field of amplitude A, propagating between two reflecting optical elements separated by an optical path length l, gets a phase change kl, i.e.:$A^* = A \exp[ikl]$, where $k = 2\pi/\lambda$, being λ the field wavelength (see Fig. 1e).

3.Interferometric antennas

By using these rules, the transmitted and reflected fields can be calculated relatively to a Michelson interferometer equipped (or not) with recycling mirror distant l from the beam splitter and having at the arm ends, l_1 and l_2 distant from the beam splitter respectively, two reflecting resonant optical devices (see Fig 2a).
The reflectance of the $\mu - th$ resonant optical cavity can be described by the complex function F_μ defined as :

$$\frac{A_{2\mu+2}}{A_{2\mu+1}} = iF_\mu = i\left|F_\mu\right| \exp\left[iArg\left(F_\mu\right)\right] \qquad (\mu = 1, 2) \tag{4}$$

Furthermore the transmittance and the reflectance of the beam splitter (recycling mirror) are indicated by t (τ) and r (ρ) respectively and they obey to the relations :

$$r^2 = t^2 = \sigma_{BS}/2 \qquad \rho^2 + \tau^2 = \sigma_R \tag{5}$$

The fields propagating into the interferometer are shown in detail in Fig.2a and applying the S-matrix method ,calculations lead to the final result for the reflected A_R and transmitted A_T amplitudes :

$$\begin{aligned} \frac{A_R}{A_{IN}} &= i\frac{\rho + \sigma_R T}{1 + \rho T} \\ T &= \exp\left[ik2\left(l + l_1\right)\right]\left(t^2 F_1 - r^2 F_2 \exp\left[ik2\left(l_2 - l_1\right)\right]\right) \end{aligned} \tag{6}$$

$$\begin{aligned} \frac{A_T}{A_{IN}} &= -\frac{rt\tau U}{1 + \rho T} \\ U &= \exp\left[ik\left(l + 2l_1\right)\right]\left(F_1 + F_2 \exp\left[ik2\left(l_2 - l_1\right)\right]\right) \end{aligned} \tag{7}$$

It is trivial to deduce from the relations (6) and (7) the expressions relative to the case without recycling putting $\rho = 0, \tau = 1$ and $l = 0$.
By the expressions (6) and (7) the Michelson interferometer working conditions can be fully analyzed.

The dark fringe operating point requires $A_T = 0$,i.e. $U = 0$. In the ideal condition, having the reflecting elements equal reflectance ($F_1 = F_2$), the well known Fresnel relation is deduced :

$$l_2 - l_1 = (2n+1)\frac{\lambda}{4} \quad (n = 0, 1, 2...) \tag{8}$$

Furthermore the recycling condition requires $A_R = 0$ or $\rho + \sigma_R T = 0$.
Again in the hypothesis of equal reflectance condition,i. e. : $F_1 = F_2 \equiv F = |F| \exp[iArg(F)]$, at the resonance we have ($Arg(F) = \pi$), i.e. $F = -|F|$ and the full recycling condition becomes :

$$\rho - \sigma_{BS}\sigma_R |F| \exp[ik2(l + l_1)] = 0 \tag{9}$$

This complex equation is fulfilled by putting the real and imaginary parts equal zero. The imaginary equation supplies the so called resonant recycling condition : ($l + l_1 = m\lambda/2$), ($m = 1, 2...$),then the real equation gives the condition:

$$\rho = \sigma_{BS}\sigma_R |F| \tag{10}$$

In conclusion the recycling conditions are fulfilled by matching the recycling mirror distance l at the resonant value and by setting up the recycling mirror reflectance in order to match the $\sigma_{BS}\sigma_R |F|$ value.
The performance of the Michelson intereferometer with recycling is measured quantitatively by the recycling factor, defined as the ratio of the beam intensity incoming into the Michelson arms with and without the recycling mirror. By using the symbols of Fig. 2a the arm intensity without the recycling is given by the expression :

$$\left|\bar{A}_3\right|^2 = t^2 |A_{IN}|^2 \tag{11}$$

and, in the case of dark fringe and recycling matching fulfilled conditions, the intensity with recycling can be calculated as :

$$\left|\bar{A}_3\right|^2 = |A_{IN}|^2 \frac{t^2\sigma_R}{1-\sigma_R\sigma_{BS}^2\,|F|^2} \tag{12}$$

therefore the recycling factor expression becomes :

$$Recy.Fact. = \eta_R = \frac{\sigma_R}{1-\sigma_R\sigma_{BS}^2\,|F|^2} \tag{13}$$

It is apparent that, apart the minimization of the energy losses in the recycling mirror and in the beam splitter, the recycling factor is in general mainly dependent on $|F|$, the reflectance absolute value of the resonant optical elements placed at the interferometer arm ends.
As far as the resonant elements placed at the Michelson interferometer arm ends are concerned, the Fabry-Perot (FP) optical cavity is discussed, being the case of interest of the VIRGO and LIGO projects.
A d_0 long FP optical cavity is considered (see the diagram of Fig. 2b), having mirror reflectivities r_1^2 and r_2^2 respectively (again the standard relations hold: $r_i^2 + t_i^2 = \sigma \quad (i = 1, 2)$ and $\sigma = 1 - \varepsilon^2$, assuming that the energy-losses into two mirrors to be quite similar).
It is useful to recall the relation between the FP resonant frequency ν_0 and its optical length[17,18] :

$$\nu_0 = \frac{c}{2d_0}\left[q + \frac{\Psi\left(d_0, R_i\right)}{\pi}\left(1 + m' + n'\right)\right] \tag{14}$$

where q, m' and n' are integer numbers related the longitudinal and transverse resonant modes of the cavity and Ψ is a function depending on the mirror geometry (R_i being the curvature radius of the $i-th$ mirror).
From (14) it is apparent that the optical length variation $\Delta d = d - d_0$ implies a frequency variation $\Delta\nu = \nu - \nu_0$ and conversely.

$$\frac{\Delta\nu}{\nu_0} = -\frac{\Delta d}{d_0} * \tag{15}$$
$$* \left[1 + \frac{1 + m' + n'}{\pi q + (1 + m' + n')\arccos\left(\sqrt{g_1 g_2}\right)} \frac{g_1 + g_2 - 2g_1 g_2}{2\sqrt{g_1 g_2 (1 - g_1 g_2)}}\right] \simeq -\frac{\Delta d}{d_0}$$

where $g_i = 1 - d_0/R_i$, being R_i the i-th reflector radius.
The approximation into (15) depends on the factor $1/q$,generally a very small quantity, since q measures the number of wavelengths in the cavity length.
The (15) tells to us that phase variations due to the length variations are correlated to frequency variations and conversely.
For next calculations it is vital to know the complex function F_μ describing the $\mu - th$ FP reflectance of the Michelson interferometer.
To this purpose the A_3 (A_5) exciting field of the FP cavity is considered (see the diagram of Fig.2a), producing the reflected A_4 (A_6) and the transmitted A_7 (A_9) fields respectively.
Again applying to optical cavity mirrors the S-matrix method, the expressions of the transmitted and reflected field ratio over the incident one are deduced:

$$\frac{A_{6+\mu}}{A_{2\mu+1}} = i\frac{t_1 t_2 \exp\left[i\Delta\delta_\mu/2\right]}{1 - r_1 r_2 \exp\left[i\Delta\delta_\mu\right]} \qquad (\mu = 1, 2) \tag{16}$$

$$\frac{A_{2\mu+2}}{A_{2\mu+1}} = iF_\mu = -i\frac{\sigma r_2 \exp\left[i\Delta\delta_\mu\right] - r_1}{1 - r_1 r_2 \exp\left[i\Delta\delta_\mu\right]} = i\frac{\sigma r_2 - r_1}{1 - r_1 r_2}\sqrt{\frac{1 + (\alpha^2 - 1)\sin^2\Delta\delta_\mu/2}{1 + (\beta^2 - 1)\sin^2\Delta\delta_\mu/2}} *$$
$$\exp\left[i\left(\pi + \arctan\left(\frac{(\alpha + \beta)\tan\Delta\delta_\mu/2}{1 - \alpha\beta\tan^2\Delta\delta_\mu/2}\right)\right)\right] \simeq$$
$$i\frac{\sigma r_2 - r_1}{1 - r_1 r_2} * \exp\left[i\left(\pi + (\alpha + \beta)\Delta\delta_\mu/2\right)\right] \tag{17}$$

where the involved symbols follow the definitions :

$$\alpha = \frac{\sigma r_2 + r_1}{\sigma r_2 - r_1} \qquad \beta = \frac{1 + r_1 r_2}{1 - r_1 r_2} \tag{18}$$

$$\Delta\delta_\mu = 2k(d_\mu - d_0) = -\frac{\omega - \omega_0}{\omega_0}(q + 1/2)2\pi \tag{19}$$
$$d_0 = (q + 1/2)\lambda/2 \qquad FSR = \frac{c}{2d_0} \qquad \nu_0 = FSR\,(q + 1/2)$$

$\Delta\delta_\mu$ indicates the detuning phase from the resonant condition of the $\mu - th$ FP, d_μ is the actual length around the resonant length d_0 and ν_0 the resonant frequency defined as the *free spectral range* (FSR) of the resonant cavity times $q + 1/2$, where q is a positive integer number (for instance in the FP cavities of VIRGO project: $d_0 = 3\,10^3\,m, \nu_0 = 2.83\,10^{14}\,Hz$ it results $q = 5659999999$).
A comment is required about the fact that the second expression of $\Delta\delta_\mu$ definition is independent of μ index, despite of the fact that the phase variation in two FP can be due to wathever origin, hence in general different. The explanation is that it is supposed that the phase variation is due to common exciting field, then producing an equal effect in two cavities.
In (17) the FP reflected field is written giving the argument in explicit form both in the exact and approximate version, if a very small $\Delta\delta_\mu$ value is considered.

4.The case of the VIRGO project interferometer

It is well known that an optical cavity stores e.m. energy $E = cost * \bar{I}$, where $\bar{I}$ is the averaged intensity on the cavity optical length, and :

$$cost = \frac{interferring \quad beam \quad volume}{velocity \quad of \quad light}$$

The function $I(z)$ is evaluated by computing[19] the interference of two beams going back and forth between two mirrors distant d_0 with reflectivity r_1^2 and r_2^2 respectively :

$$I(z) = I_{IN}\frac{\sigma_1 - r_1^2}{(1 - r_1 r_2)^2}[(1 - r_2)^2 + 4r_2 \cos^2 \psi(z)/2]A_{ir} \tag{20}$$

where A_{ir} is the Airy function given by:

$$A_{ir} = [1 + \frac{2r_1 r_2}{(1 - r_1 r_2)^2}(1 + \cos(k2d_0)]^{-1} \tag{21}$$

and $\psi(z) = 2kz$ being z the current position between the mirrors.
The function $I(z)$ shows the standard interference pattern, its mean value $\bar{I}$ results :

$$\bar{I} = I_{IN}\frac{\sigma_1 - r_1^2}{(1 - r_1 r_2)^2}(1 + r_2^2)A_{ir} \tag{22}$$

The formula (22) at the resonance becomes :

$$\bar{I}_{res} = I_{IN}\frac{\sigma_1 - r_1^2}{1 - r_1 r_2}\frac{1 + r_2^2}{\pi\sqrt{r_1 r_2}}F^* \tag{23}$$

where the cavity finesse defined by the following expression has been introduced:

$$F^* = \frac{\pi\sqrt{r_1 r_2}}{1 - r_1 r_2} \tag{24}$$

In the case $r_1^2 < r_2^2 \simeq \sigma_1 \simeq 1$ the (23) becomes :

$$\bar{I}_{res} = I_{IN} 2F^* \frac{1+r_1}{\pi\sqrt{r_1 r_2}} \simeq I_{IN} \frac{4}{\pi} F^* \tag{25}$$

otherwise when $r_1^2 = r_2^2$ and $\sigma_1 \simeq 1$:

$$\bar{I}_{res} = I_{IN} F^* \frac{1+r_1^2}{\pi\sqrt{r_1 r_2}} \simeq I_{IN} \frac{2}{\pi} F^* \tag{26}$$

As an exercise it is useful to apply these formulas to Michelson interferometer. Indeed, if $A_T = 0$, the interferometer is seen as two *cavities* constituted by a common optical length l plus two branches l_1 and l_2, both having end mirror reflectivities ρ^2 and $\sigma_{BS}^2 |F|^2$ respectively. The two corresponding reflected amplitudes are:

$$\frac{A_{R\mu}}{A_{IN}} = i \frac{\rho \mp \sigma_R \sigma_{BS} |F| \exp\left(ik2(l+l_\mu)\right)}{1 \mp \rho\sigma_{BS} |F| \exp\left(ik2(l+l_\mu)\right)} \quad (\mu = 1,2) \tag{27}$$

at resonance $2k(l+l_1) = 2\pi$ with uppersign and $2k(l+l_2) = \pi$ with the lowersign, thus the average stored intensity in each cavity is at resonance:

$$\bar{I}(l+l_1) = \bar{I}(l+l_2) = A_{IN}^2 \frac{\sigma_R - \rho^2}{(1-\rho\sigma_{BS}|F|)^2}(1+\sigma_{BS}^2|F|^2) \tag{28}$$

These cavities are called *recycling cavities.*
Since the Michelson interferometer must work with $A_R = 0$,which implies $\rho = \sigma_R \sigma_{BS} |F|$, then each cavity gets an average intensity equal to :

$$\bar{I}(l+l_1) = \bar{I}(l+l_2) \simeq A_{IN}^2 \frac{1+\rho^2}{1-\rho^2} \simeq \frac{2}{\pi} F^* A_{IN}^2 \tag{29}$$

It is worth while to note that the intensity calculated in each branch supplies the following result :

$$\bar{I}(l) + \bar{I}(l_1) + \bar{I}(l_2) = \bar{I}(l+l_1) + \bar{I}(l+l_2) \tag{30}$$

We report the numerical values of the most remarkable parameters discussed above in the case of the VIRGO interferometric antenna in the matching conditions of recycling and FP resonance.
The optical element characteristics of the VIRGO antenna are listed below:

i) - Energy-losses:
the energy-losses are estimated to be of the order of 50 p.p.m. for each optical component, therefore we have :
$\sigma_R \sim \sigma_{BS} \sim \sigma \sim 1 - 50\,10^{-6}$

ii) - Reflectivities :
the recycling mirror reflectivity is $\rho^2 = .976$
the beam splitter reflectivity is $r^2 = t^2 = 1/2$
the FP entry mirror reflectivity is $r_1^2 = .975$
the FP end mirror reflectivity is $r_2^2 = 1. - 10^{-4}$
the FP resonant reflectivity is $|F|^2 = .976$
the FP resonant transmittivity is $|S|^2 = 8.1\,10^{-3}$

iii) - recycling factor is $\eta_R = 41$

iv) - cavity finesse :
recycling cavity finesse is $F_l^* = 129$
FP cavity finesse is $F_d^* = 259$

v) - geometrical lengths :
recycling mirror beam splitter distance is $l = 5.m$
beam splitter FP entry mirror distance is $l_1 = l_2 = 5.m$

Given a laser source of total radiant power P_0, the intensity distribution on the beam at radius r from the beam axis expressed as :

$$P(r) = \int_0^r I_0 \exp\left(-\frac{2r'^2}{w_0^2}\right) 2\pi r'\, dr' = I_0 \frac{\pi w_0^2}{2}\left[1 - \exp\left(-\frac{2r^2}{w_0^2}\right)\right] \tag{31}$$

the (31) gives also the total power related to the intensity I_0 in the limit $r \to \infty$:

$$I_0 = P_0 \frac{2}{\pi w_0^2} \tag{32}$$

Suppose, as in the VIRGO project case, to have a laser source of power $P_0 = 10\,W$, feeding the Michelson interferometer with recycling, the matching condition with a beam waist diameter $2w_0 = 4\,10^{-2} m$ supplies an incoming intensity $I_{IN} = 2\,10\,(2\,10^{-2})^{-2}/\pi = 1.6\,10^4\,Wm^{-2}$. Hence the following typical quantities can be evaluated :

i) - <u>energy stored into the recycling cavity</u> :
$E_{RC} \simeq \frac{2}{\pi} F_l^* \left|A_{IN}\right|^2 * V/c = \frac{2}{\pi} F_l^* P_0 2l/c = .64 * 129 * 10 * 2 * 10/(3\,10^8) = 5.5\,10^{-5}\,J$
where il volume V is defined as $V = \pi w_0^2 (l + l_1)$.

ii) - <u>intensity of the beam impinging the FP cavity</u> :
$\left|A_3\right|^2 = t^2 \eta_R \left|A_{IN}\right|^2 = 3.3\,10^5\,W\,m^{-2}$

$\left|A_5\right|^2 = r^2 \eta_R \left|A_{IN}\right|^2 = 3.3\,10^5\,W\,m^{-2}$
with $t^2 = r^2 = 1/2$

iii) - <u>energy stored into each FP cavity</u> :
$E_{FP} \simeq \frac{4}{\pi} F_d^* \eta_R \left|A_{IN}\right|^2 \frac{1}{2} V/c = \frac{2}{\pi} F_d^* \eta_R P_0 2 d_0/c = .64 * 259 * 41 * 10 * 2 * 3 * 10^3/3\,10^8 = 1.35\,J$
where il volume V is defined as $V = \pi w_0^2 d_0$

iv) - <u>beam intensity transmitted by the FP end mirror</u> :
$\left|A_7\right|^2 = \left|A_8\right|^2 = \left|S\right|^2 \eta_R \left|A_{IN}\right|^2 t^2 = 2.6\,10^3\,Wm^{-2}$

5.Broad band interferometric antenna sensitivity

This section is devoted to discuss the recycling Michelson interferometer sensitivity in detecting GW in a broad region of frequency.
It is well known that the GW effect on the interferometer test masses[20], which are the mirrors of two FP cavities, consists in an equal and opposite length variation $\Delta d_\mu = (-1)^\mu (d - d_0) = (-1)^\mu \Delta d$ of two FP's placed along the orthogonal arms of the interferometer (see ref.3).
According to the formulae (7) and (17) these length variations produce a total phase variation of $2\Delta\delta = 4k(d - d_0)$ in the transmitted intensity expressed by the following relation :

$$\frac{\Delta I_T}{I_{IN}} \equiv \frac{|A_T(\Delta\delta \neq 0)|^2 - |A_T(\Delta\delta = 0)|^2}{|A_{IN}|^2} = \tag{33}$$

$$\frac{\sigma_{BS}^2 (\sigma_R - \rho^2) |F|^2 C_+/2}{1 + \rho^2 \sigma_{BS}^2 |F|^2 C_-/2 + 2\rho\sigma_{BS} |F| \sin[\psi_R + \psi_M/2] \sin[(\alpha + \beta)\Delta/2 - \psi_M/2]}$$

where :

$$C_\pm = 1 \pm \cos[(\alpha + \beta)\Delta\delta + \psi_M]$$
$$\psi_M = k2(l_1 - l_2) \qquad \psi_R = k2(l + l_1) \tag{34}$$

Putting into the (33) the working condition at the extinction (8) and the recycling conditions (9) and (10), with a good degrees of accuracy the ΔI_T expression becomes (an exhaustive discussion of the whole optical system is given in Appendix-C) :

$$\frac{\Delta I_T}{I_{IN}} \simeq \frac{\sigma_{BS}^2 \sigma_R}{2} |F|^2 \frac{1 - \cos[(\alpha + \beta)\Delta\delta]}{1 - \sigma_R \sigma_{BS}^2 |F|^2} = \sigma_{BS}^2 |F|^2 \eta_R \Delta\Phi^2 \tag{35}$$

where the phase $\Delta\Phi$,considered as a small quantity, is given by the expression :

$$\Delta\Phi = (\alpha + \beta)\frac{\Delta\delta}{2} \simeq \frac{F^*}{\pi}\sqrt{\frac{r_2}{r_1}}\frac{1 - r_1^2}{r_2 - r_1}\Delta\delta \tag{36}$$

Into the (36) the finesse parameter has been introduced and the reasonable approximation $\sigma \simeq 1$ has been performed.
In the case of interferometric antennas the reflectance $r_2^2 \simeq 1$, then the expression (36) becomes :

$$\Delta\Phi \simeq \frac{F^*}{\pi}\frac{1+r_1}{\sqrt{r_1}}\Delta\delta = \frac{F^*}{\pi}\frac{1+r_1}{\sqrt{r_1}}2k\Delta d = \frac{F^*}{\pi}\frac{1+r_1}{\sqrt{r_1}}\frac{2d_0}{c}\Delta\omega \simeq \frac{8F^*\Delta d}{\lambda} \quad (37)$$

having expressed the phase $\Delta\delta$ by means of the optical length and frequency variation[21].
By using a standard technique the transmitted intensity is phase-modulated at high frequency ($\sim 10\,MHz$) in order to get a signal at first order and to minimize the noisy effects of the laser fluctuations.
In the following calculation the external phase-modulation case is considered[22]; i.e. the transmitted field before the photodiode detection is undergone to interference with a small fraction of the main field A_0 phase-modulated at high frequency by means of an electro-optic device.
After photodiode detection, the output current signal is demodulated and low-pass filtered with a frequency band Δf.
The final current signal is shot noise limited and the signal to noise ratio[23] (SNR) can be obtained (see for detail of this calculation the Appendix-A) :

$$SNR = \sqrt{2}J_1(m)\,\sigma_{BS}\,|F|\sqrt{\frac{2\eta I_0\eta_R}{h\nu_0}}\frac{\Delta\Phi}{\sqrt{\Delta f}} \quad (38)$$

where $h\nu_0$ is the photon energy, η the photodiode quantum efficiency and $J_1(m)$ is the Bessel function relatively to the modulation amplitude m.
The SNR expression given by (38) depicts the sensitivity of the recycling interferometer in detecting a phase $\Delta\Phi$ given by (36). It is important to point out that the expression (38) is a "stationary picture", because nothing is told about the time dependence of the phase $\Delta\Phi$.
In order to get the interferometer sensitivity relatively to the case of a <u>harmonic modulation</u> of the optical length around its resonant value d_0, a different approch is needed in handling the resonant cavity.
This approch concerns the description of the resonant cavity in term of energy fluxes.

In fact following this line, the resonator behaviour is given in term of general parameters like the resonance frequency, the storage time and the Q-factor, hence each resonator is described in the quite similar way, no matter if it is a "LC" circuit or an optical cavity.
But the general parameters are expressed in terms of different components describing the particular resonator.
According to the ref.16, in a "LC" resonator the reflected over incident intensity is given by the formula :

$$\frac{I_R}{I_{IN}} = \left[\frac{\tau}{\bar{\tau}}\right]^2 \frac{1+\delta^2\bar{Q}^2}{1+\delta^2 Q^2} \tag{39}$$

where $\delta = (\omega - \omega_0)/\omega_0, Q = \omega_0\tau$ and $\bar{Q} = \omega_0\bar{\tau}$. The parameters τ and $\bar{\tau}$ are given by the following definitions :

$$\frac{1}{\tau} = \frac{1}{\tau_e} + \frac{1}{\tau_0} \qquad \frac{1}{\bar{\tau}} = \frac{1}{\tau_e} - \frac{1}{\tau_0} \tag{40}$$

where τ_e is the decay time relative to the external energy-losses (escaping energy fluxes) and τ_0 the decay time relative to the internal energy-losses (energy lost in the elements) of the resonator.
In the case of an optical resonant cavity the reflected over the incident intensity ratio can be deduced from the formula (17) taking into account that, since the *free spectral range* (FSR) is larger than the cavity width ($FSR >> FWHM$), it is allowed the approximation :
$\sin[2d_0(\omega-\omega_0)/2c] \simeq 2d_0(\omega-\omega_0)/2c$:

$$\left|\frac{A_{2\mu+2}}{A_{2\mu+1}}\right|^2 \simeq \left(\frac{\sigma r_2 - r_1}{1-r_1 r_2}\right)^2 \frac{1+(\alpha^2-1)\left[2d_0(\omega-\omega_0)/2c\right]^2}{1+(\beta^2-1)\left[2d_0(\omega-\omega_0)/2c\right]^2} =$$
$$\left(\frac{\sigma r_2 - r_1}{1-r_1 r_2}\right)^2 \frac{1+[\frac{2d_0\sqrt{\sigma r_1 r_2}}{c(\sigma r_2 - r_1)}]^2(\omega-\omega_0)^2}{1+[\frac{2d_0\sqrt{r_1 r_2}}{c(1-r_1 r_2)}]^2(\omega-\omega_0)^2} \tag{41}$$

The formulae (39) and (41) show the same structure and it is straightforward to point out the same meaning of the corresponding terms :

$$\tau = \frac{2d_0}{c}\frac{\sqrt{r_1 r_2}}{1 - r_1 r_2} \qquad \bar{\tau} = \frac{2d_0}{c}\frac{\sqrt{\sigma r_1 r_2}}{\sigma r_2 - r_1} \tag{42}$$

the Q-factor and the δ parameters get a quite similar significance.
Now the differential equations describing the resonator fields can be modified taking into account the effect of a small harmonic perturbation $p(t) = p\cos[\Omega t]$ affecting the optical length or correspondently the field frequency. By looking for a first order solution in the perturbation amplitude p, the reflected amplitude is given by the following expression (see for detail the Appendix-B) :

$$S_-(t) = \frac{\tau}{\bar{\tau}}\exp[i\omega t]\left[\frac{1 - i\delta\bar{Q}\sqrt{\sigma}\bar{\tau}/\tau}{1 + i\delta Q} - \right. \tag{43}$$
$$\left. p\frac{iQ}{1 + i\delta Q}\frac{\exp[i\Omega t]}{1 + i\delta_+ Q} - p\frac{iQ}{1 + i\delta Q}\frac{\exp[-i\Omega t]}{1 + i\delta_- Q}\right] \equiv CR - SB_+ - SB_-$$

the amplitude (43) describes a carrier field (CR) and two side bands (SB_+ and SB_-), generated by the perturbation $p(t)$, of frequency $\nu_+ = \nu + \Omega/2\pi$ and $\nu_- = \nu - \Omega/2\pi$ respectively ($\delta_\pm = \nu_\pm/\nu_0 - 1$).
The phase $\Delta\Phi(\nu_g)$ of the reflected field[14] at the resonance ($\delta = 0$) is :

$$\Delta\Phi(\nu_g) = \frac{2|SB|}{|CR|} = 2p\frac{\omega_0\tau}{\sqrt{1 + \Omega^2\tau^2}} \tag{44}$$

if the perturbation is a gravitational wave the (43) and (44) expressions get the form we ecounter in the gravitational physics literature[3] with the symbols: $p \equiv h$, $\Omega/2\pi \equiv \nu_g$ and $(2\pi\tau)^{-1} \equiv \nu_g^0$.
Calculation of SNR leads to the following "dynamical SNR expression", where the frequency ν_g of the harmonic perturbation is present :

$$SNR = \sqrt{2}J_1(m)\,\sigma_{BS}\,|F|\sqrt{\frac{2\eta I_0\eta_R}{h\nu_0}}S(\nu_g)\frac{h}{\sqrt{\Delta f}} \tag{45}$$
$$S(\nu_g) = \frac{2\nu_0/\nu_g^0}{\sqrt{1 + \left(\nu_g/\nu_g^0\right)^2}}$$

It is straightforward to verify that the expression (45) goes into the "stationary form" (38) if ν_g is put equal zero.
In fact, reminding that the gravitational perturbation amplitude can be given as $h = \Delta d/d_0$ and using the formula (42), it results :

$$2h\frac{\nu_0}{\nu_g^0} = 2\frac{\Delta d}{d_0}2\pi\nu_0\tau = 2\frac{\Delta d}{d_0}2\pi\nu_0\frac{2d_0}{c}\frac{\sqrt{r_1 r_2}}{1-r_1 r_2} = \frac{F^*}{\pi}2k2\Delta d \simeq \Delta\Phi$$

which is the $\Delta\Phi$ definition given in the formula (36) in the approximation $(1+r_1)/\sqrt{r_1} \approx 2$.
It is also apparent from the expression (45) that the only effect of the recycling is to enhance the power I_0 by the factor η_R.
The (45) gets the frequency dependence through the function $S(\nu_g)$, which is a *low-pass filter-like* function, having the cut frequency at ν_g^0.
It is interesting to plot the function $S(\nu_g)$ in the VIRGO project case at different cut frequency ν_g^0 in the recycling ($\eta_R > 1$) and without recycling ($\eta_R = 1$) cases.(See in Fig. 4 the curves of the function $S(\nu_g)\sqrt{\eta_R}/\nu_0$)
The meaning of the curve labels given in Fig.4 are defined in TABLE I; they correspond at different frequency cut ν_g^0, finesse F^* and recycling factor η_R by parametrizing the reflectivity r_1^2 of the FP front mirror.
The curves of Fig. 4 tell to us that in the high frequency range of the perturbation, at low finesse values, a remarkable advantage is got by using the recycling technique, on the contrary, in the low frequency range of the perturbation at high finesse values, the recycling use is of scarce usefulness.

TABLE I

	$\sqrt{\eta_R}$	r_1^2	F^*	ν_g^0 (Hz)	τ (msec)
a	1	.14	3.	5.10^3	$3.2\,10^{-2}$
a^*	40.	.14	3.	5.10^3	$3.2\,10^{-2}$
b	1	.85	37.	676.	.16
b^*	17.8	.85	37.	676.	.16
c	1	.975	247.	100.	1.6
c^*	5.6	.975	247.	100.	1.6
d	1	.995	1200.	20.	8.
d^*	2.5	.995	1200.	20.	8.

6.Narrow band version of the interferometric antenna

So far an interferometric antenna has been discussed having a broad band sensitivity (see Fig. 4), in particular a flat frequency response below the cut frequency ν_g^0 and a suppressing behaviour at frequency higher than ν_g^0.
In this section a different version of an interferometric antenna is presented, using an optical arrangement capable of giving a tunable narrow band sensitivity.
This method, originally proposed by Drever[6] (1983), has been studied successively in a complet theory by Vinet[9] (1986).
The Drever's idea is based on the symmetric coupling of two long cavities of a Michelson interferometer arms with a short cavity, by settling the recycling mirror beyond the beam splitter (see the optical arrangement in Fig. 5a).
As extensively described in Appendix-D, this symmetric system made of three coupled cavities (the symmetry involves the optical path lengths as well as the reflectivities of the optical elements) shows two resonant oscillation modes at the circular frequencies ω_S and ω_A, where the labels indicate the character symmetric and antisymmetric of the longitudinal oscillation modes of the optical system.
The narrow band behaviour of the antenna is reached *by matching the laser frequency on the symmetric or antisymmetric resonant mode*, then the antenna sensitivity becomes resonant at a gravitational perturbation frequency equal to the difference of two resonat modes of the coupled cavities.
In the following this mechanism is described in detail. By referring to the Fig. 5a, the feeding laser field A_0 is shared in two fields by means of the beam splitter of reflectivity r^2 and transmittivity t^2, being $r^2 = t^2 = \sigma_{BS}/2$.
These two fields are converging through two symmetric optical paths l_1 and l_2 on the recycling mirror, which gives access to the optical short cavity of total path length a.
The two long FP optical cavities along the interferometer arms are defined by the front and end mirrors at a distant d_0 with reflectivities r_1^2 and r_2^2 respectively.
Of course, by the symmetry of the optical lay out, back to beam splitter, two similar fields, the reflected and the transmitted ones, are present.
In the reasonable hypothesis that the corner mirrors along the paths l_μ ($\mu = 1, 2$) get an almost unitary reflectivity ($r_c^2 \simeq 1$), the two fields $A_{0\mu}$

reaching the recycling mirror of reflectivity ρ^2 and transmittivity τ^2 get the form :

$$
\begin{aligned}
A_{01} &= ir_c ir A_0 \exp(ikl_1) \simeq -rA_0 \exp(ikl_1) \\
A_{02} &= ir_c t A_0 \exp(ikl_2) \simeq itA_0 \exp(ikl_2)
\end{aligned} \tag{46}
$$

The field configurations originated by two incoming fields A_{01} and A_{02} propagating into the optical system are shown in Fig 5b and 5c separately for semplicity sake, but, of course, they are to be considered superimposed.
By applying the S-matrix method to these configurations one obtains back from the recycling mirror four fields $A_{T\mu}$ and $A_{R\mu}$ having the expression :

$$
\begin{aligned}
A_{T\mu} &= iA_{0\mu} \frac{\tau^2 F_\mu \exp(ika)}{1 - \rho^2 F_1 F_2 \exp(ik2a)} = iA_{0\mu} X_\mu \\
A_{R\mu} &= iA_{0\mu} \rho \frac{1 - F_1 F_2 \exp(ik2a)}{1 - \rho^2 F_1 F_2 \exp(ik2a)} = iA_{0\mu} Y
\end{aligned} \tag{47}
$$

where F_μ is the complex parameter describing the reflectance of the $\mu - th$ FP optical cavity and holding the definitions :

$$
X_\mu = \frac{\tau^2 F_\mu \exp(ika)}{1 - \rho^2 F_1 F_2 \exp(ik2a)} \qquad Y = \rho \frac{1 - F_1 F_2 \exp(ik2a)}{1 - \rho^2 F_1 F_2 \exp(ik2a)} \tag{48}
$$

The $\mu = 1$ ($\mu = 2$) case corresponds to the diagram of Fig. 5b (5c).
It is straightforward to deduce the resulting transmitted field back to beam splitter :

$$
\begin{aligned}
A_T &= t(A_{T1} + A_{R2}) \exp(ikl_1) + ir(A_{R1} + A_{T2}) \exp(ikl_2) = \\
& rtA_0 [X_1 \exp(ik2l_1) + X_2 \exp(ik2l_2)] + \\
& iA_0 \sigma_{BS} \left[r^2 - t^2\right] Y \exp[ik(l_1 + l_2)]
\end{aligned} \tag{49}
$$

the term in Y of (49) vanishes by using the given condition $t^2 = r^2 = \sigma_{BS}/2$.
From (49) the intensity of the transmitted beam can be deduced :

$$\frac{|A_T|^2}{|A_0|^2} = r^2t^2\left|X_1\exp\left[ik2l_1\right] + X_2\exp\left[ik2l_2\right]\right|^2 = \tag{50}$$

$$r^2t^2\tau^4\left|F\right|^2\frac{2 + (\exp\left[i(Arg[F_1] - Arg[F_2] + k2(l_1 - l_2))\right] + cc)}{1 + \rho^4\left|F\right|^4 - \rho^2\left|F\right|^2(\exp\left[i(Arg[F_1] + Arg[F_2] + k2a)\right] + cc)}$$

By referring to the formulae (17) and (36), in the case of GW perturbation it results that $\Delta\Phi_1 = -\Delta\Phi_2 = \Delta\Phi = q\Delta\omega 2d_0/c$, hence $Arg[F_1] - Arg[F_2] = 2\Delta\Phi$. On the other hand by using the energy flux conservation (see formula (7) of Appendix-D with the condition $\gamma = 1$), one obtains $Arg(F_1) + Arg(F_2) + \phi = 2\pi\ mod(2\pi)$, hence the (50) becomes:

$$\frac{|A_T|^2}{|A_0|^2} = 2r^2t^2\tau^4\left|F\right|^2\frac{1 + \cos\left[2\Delta\Phi + k2(l_1 - l_2)\right]}{(1 - \rho^2\left|F\right|^2)^2} \tag{51}$$

Putting into the (51) the values of $r^2 = t^2 \simeq 1/2$ as well as the extinction condition, the (51) takes the form :

$$\frac{|A_T|^2}{|A_0|^2} = \frac{(1-\rho^2)^2\left|F\right|^2}{(1 - \rho^2\left|F\right|^2)^2}\sin^2\Delta\Phi \tag{52}$$

The result (52) is analogous to the broad band case of the interferometer discussed above and given by the formulae (35) and (36).
However it is important to point out the difference of this case. In fact, as will be clear by the following argumentations, in the narrow band optical system the *stationary case* doesn't exist by definition.
In order to calculate the relaxation times of the optical system, the same procedure followed in the broad band case will be adopted.
The original expression (47) of the transmitted field $A_{T\mu}$ is considered. Since the phase effects are given by the exciting field $A_{0\mu}$ and therefore equal into the two long cavities, it is allowed to put $F_1 = F_2 = |F|\exp(iArg[F])$.
Thus the transmitted intensity is given by the expression :

$$\frac{|A_{T\mu}|^2}{|A_{0\mu}|^2} = \frac{\left|\tau^2F_\mu\exp(ik2a)\right|^2}{\left|1 - \rho^2\left|F\right|^2\exp(i2Arg[F])\exp(ik2a)\right|^2} \tag{53}$$

the result (53) can be written in the following form directly comparable with the expression (22) of Appendix-B:

$$\frac{|A_{T\mu}|^2}{|A_{0\mu}|^2} = \left[\frac{(1-\rho^2)\,|F|}{1-\rho^2\,|F|^2}\right]^2 * \frac{1}{1+\left[(\omega-\omega_0)(\alpha+\beta)(2d_0/c)\rho\,|F|\,/(1-\rho^2\,|F|^2)\right]^2} \tag{54}$$

The relaxation time constant τ^* results defined as :

$$\tau^* = \frac{\rho\,|F|}{1-\rho^2\,|F|^2}\Theta \tag{55}$$

$$\Theta = \frac{2d_0}{c}\,(\alpha+\beta) = \frac{2d_0}{c}\,\frac{2r_2(\sigma-r_1^2)}{(\sigma r_2 - r_1)(1-r_1 r_2)}$$

The value of the time constant Θ is roughly four times τ ($\Theta \approx 4\tau$) in the reasonable approximations $\sigma \simeq r_2^2 \simeq 1$, $\sqrt{r_2/r_1} \approx 1$ and $\sqrt{\sigma} + r_1 \approx 2$.
On the base of the transmitted field expression (23) of Appendix-B relative to the harmonic perturbation $h(t) = h\cos(\Omega t)$ of a resonator connected to two guides, the analogous expression of the field transmitted by the three coupled cavities can be written. However the existence of two resonant modes allows to performe a choice. In the case of exciting the ω_A mode the following parameter definitions are to be considered:

$$\begin{aligned}
&\omega_\pm = w \pm \Omega \\
&\gamma_A = \frac{1}{\tau^*} - j\omega_A \qquad \gamma_S = \frac{1}{\tau^*} - j\omega_S \\
&Q_S = \omega_S\tau^* \qquad Q_A = w_A\tau^* \qquad \delta = \frac{\omega-\omega_A}{\omega_A} \\
&\delta_+ \equiv \delta_S = \frac{\omega+\Omega-\omega_S}{\omega_S} \qquad \delta_- \equiv \delta_A = \frac{\omega-\Omega-\omega_A}{\omega_A}
\end{aligned} \tag{56}$$

Thus the perturbed transmitted field gets the expression :

$$S_-(t) = S_0 \frac{k_2^2 2\tau^*}{1 + j\delta Q_A} [\exp(j\omega t) - \tag{57}$$
$$h\tau^* \left(\frac{\gamma_S \exp(j\omega_+ t)}{1 + j\delta_S Q_S} + \frac{\gamma_A \exp(j\omega_- t)}{1 + j\delta_A Q_A} \right) \Bigg] \equiv CR - SB_+ - SB_-$$

At the resonance $\omega = \omega_A$ the parameters get the values : $\delta = 0$, $\delta_A = -\Omega/\omega_A$ and $\delta_S = (\omega_A - \omega_S + \Omega)/\omega_S$. In particular δ_S vanishes for $\bar{\Omega} = \omega_S - \omega_A$. That means that the transmitted field gets a peaked behaviour at the frequency $\bar{\omega}_+ = \omega_A + \bar{\Omega}$ due to term SB_+. The other perturbation term SB_- remains actually limited and doesn't play any role in the narrow band mechanism.
That can be seen quantitatively by looking at the phase $\Delta\Phi(\nu_g)$ defined in the present case as (see Appendix-B) :

$$\Delta\Phi(\nu_g) = \frac{|SB_+|}{|CR|} = h \left| \frac{1 - j\omega_S \tau^*}{1 + j\delta_S Q_S} \right| \tag{58}$$

at the resonance ($\omega = \omega_A$) the phase (58) becomes:

$$\Delta\Phi(\nu_g) = h \sqrt{\frac{1 + (\omega_S \tau^*)^2}{1 + (\omega_A - \omega_S + \Omega)^2 \tau^{*2}}} \simeq$$
$$h \frac{\nu_S 2\pi\tau^*}{\sqrt{1 + (\nu_A - \nu_S + \nu_g)^2 (2\pi\tau^*)^2}} \tag{59}$$

By using the result (55) : $\tau^* \simeq \tau 4\rho\,|F|\,/(1 - \rho^2\,|F|^2)$ together with the relation $\nu_S - \nu_A = 1/\pi\tau$ given in Appendix-D, the expression (59) can be put in the form :

$$\Delta\Phi(\nu_g) = h\eta_E \frac{\nu_S/\nu_g^0}{\sqrt{1 + \eta_E^2((\nu_g - \nu_g^0)/\nu_g^0)^2}} \tag{60}$$

where the cut frequency $\nu_g^0 \equiv 1/\pi\tau$ gets a different definition with respect to the previous definition of the broad band case and an *expansion factor* η_E is

defined as :

$$\nu_g^0 = \nu_S - \nu_A = \frac{c}{2\pi d_0} \arctan\left(\frac{1-r_1^2}{2r_1 \sin\phi/2}\right) \qquad \eta_E = \frac{8\rho\,|F|}{1-\rho^2\,|F|^2} \tag{61}$$

Let us go back to the expression (51) of the transmitted intensity in the form :

$$\frac{|A_T|^2}{|A_0|^2} = 2t^2r^2 \frac{\tau^4\,|F|^2}{(1-\rho^2\,|F|^2)^2}\left[1+\cos\left(2\Delta\Phi(\nu_g)+k2(l_1-l_2)\right)\right] \tag{62}$$

it is worth while to remark that the cosinus argument is the sum of two terms, each being characterized by the frequency ν_S and ν_A respectively.
In fact the phase $\Delta\Phi(\nu_g)$ is carried by the frequency ν_S as it is obvious from the expression (62) and the factor k of the second term has to be defined as $k = \omega_A/c$ accordingly with the laser frequency matching the frequency ν_A.
Therefore the transmitted intensity depends on two frequencies ν_A and ν_S, but the settling of the Michelson interferometer at the extinction eliminates the component at frequency ν_A, leaving the transmitted intensity at the frequency ν_S.
If a hetherodyne detection is performed between the carrier ν_A and the side band ν_S, one obtains a signal proportional to:

$$\begin{aligned} &|A_T| = |A_0|\,hS(\nu_g) = \\ &|A_0|\,h\frac{(1-\rho^2)\,|F|}{(1-\rho^2\,|F|^2)}\frac{\eta_E\nu_S/\nu_g^0}{\sqrt{1+\eta_E^2((\nu_g-\nu_g^0)/\nu_g^0)^2}} \end{aligned} \tag{63}$$

where $S(\nu_g)$ gets the same meaning as in the broad band case; if $\rho^2 = |F|^2$ the (63) supplies the following expression for $S(\nu_g)$:

$$S(\nu_g) = \frac{\eta_E}{2}\frac{\nu_S/\nu_g^0}{\sqrt{1+\eta_E^2((\nu_g-\nu_g^0)/\nu_g^0)^2}} \tag{64}$$

In Fig. 6 the (64) is plotted for different values of the phase ϕ ($\phi = \pi, \pi/3, \pi/6$ and $\pi/9$) corresponding to the frequencies $\nu_g^0 \simeq 40, 80, 154$ and $230\,Hz$ respectively. The curves shown in Fig. 6 are computed for the following set of values:

$$r_1^2 = .995 \qquad r_2^2 = .99999 \qquad \sigma = .999995$$

Finally a relevant problem arises about the scientific use of the narrow band gravitational antenna.

The problem concerns how low in frequency can be tuned the antenna. That is directly connected to the detection of gravitational periodic signals emitted by rotating neutron stars, whose frequency spectrum is located to low frequency ($3\,Hz$).

As it is shown in Appendix-D (see formula (18)) the frequency difference of two resonant modes,corresponding to the minimim tunable frequency of antenna, is reached by doing the minimum coupling between the long cavities ($\phi = \pi$). It results that the minimum tunable frequency is of the order of the cavity FSR times the factor $1 - r_1^2$, therefore the narrow band optics of the antenna requires high values of the front mirror reflectivity, or high finesse[16] of the long cavities.

Another limitation of the minimum tunable frequency could be given by the widths of resonant peaks.

However it has been shown that such a width is ν_g^0/η_E, therefore, as the peak position ν_g^0 is moved more and more down in frequency, the ratio of the width over the peak position is constant and equal to $1/\eta_E$. Hence the tuning of antenna in the low frequency limit results remarkable favorable.

7.Validity conditions of sensitivity formulas

It has been undoubtedly noticed that the conditions $r_1^2 < r_2^2 \simeq \sigma \simeq 1$ has been widely used throughout the paper. That is due to the fact that these inequalities are the standard settling of the long FP optical cavities of a GW interferometer detector.
Besides these conditions are directly tied to the condition $|F|^2 \simeq 1$, which is to the base of most important results presented in this paper and it is also connected to the frequency cut ν_g^0, which characterizes the frequency range where the antenna is capable to detect GW with good efficiency.
Hence in this section the validity limits of these conditions are discussed.
By defining the characteristic time constants $\tau_{FSR}, \tau^{'}$ and $\tau^{"}$ as :

$$\tau_{FSR} = \frac{2d_0}{c} \quad \tau^{'} = \frac{2d_0}{c}(1 - r_1 r_2)^{-1} \quad \tau^{"} = \frac{2d_0}{c}(1 - \sqrt{\sigma} r_2)^{-1} \tag{65}$$

the conditions $r_1^2 < r_2^2 \simeq \sigma \simeq 1$ imply the following inequalities:

$$\tau_{FSR} < \tau^{'} < \tau^{"} \tag{66}$$

Following the adimensional notations $t_m = \tau_{FSR}/\tau^{"}$ and $t = \tau^{'}/\tau^{"}$, used in the Vinet's paper[8], the (66) corresponds to the inequalities :

$$t_m < t < 1 \tag{67}$$

At the resonance of the FP cavity the expression of $|F|^2$ can be written as function of t and t_m:

$$|F|^2 = \left(\frac{\sigma r_2 - r_1}{1 - r_1 r_2}\right)^2 = \left(\frac{1 + t t_m - 2t}{r_2}\right)^2 \simeq (1 - 2t)^2 \tag{68}$$

being the approximation in (68) allowed by the smallness of t_m .
It is clear from (68) that the validity of the approximation $|F|^2 \simeq 1$ depends on the smallness of $t = (1 - \sqrt{\sigma} r_2)/(1 - r_1 r_2)$ with respect to unit.
Since $r_2^2 \simeq \sigma \simeq 1$, that, in turn, depends on the value of r_1^2 or, if you want, on the choice of the finesse F^*.

That becomes apparent by showing the t dependence on the different parameters :

$$t = \frac{\tau'}{\tau''} = \frac{1}{\tau''}\frac{1}{2\pi\nu_g^0} = \frac{1-\sqrt{\sigma}r_2}{1-r_1r_2} = \frac{1-\sqrt{\sigma}r_2}{\pi\sqrt{r_1r_2}}F^* \tag{69}$$

By using the numerical values of section 4 : $r_2^2 = 1-10^{-4}$ and $\sigma = 1-50\,10^{-6}$, it results that $\tau'' = .2666\,sec$ and $t = .597/\nu_g^0$.
This function is plotted versus ν_g^0 in Fig.9, and two more horizontal scales are added reporting the corresponding values of the reflectivity r_1^2 and the finesse F^*.
The Fig.9 shows that in the finesse range so far considered for the interferometric antennas ($20 < F^* < 400$) the condition $|F|^2 \simeq 1$ is fairly well fulfilled ($t \leq 10^{-2}$).
We point out that ν_g^0 is also limited at high frequencies, because it is required to be a small fraction of the free spectral range (for instance in the VIRGO case $\nu_{FSR} = 50\,KHz$).

Appendix-A

This appendix is devoted to deduce the expression of the signal to noise ratio (SNR) of the intereferometer in the case the technique of the external modulation is used.

In Fig. 3 the considered optical lay out is shown : the intereferometer is represented as a black box excited by a field A_{IN}, giving in output the transmitted field A_T. Furthermore the interferometer is supposed to work at the extinction.

As represented in the figure, the external modulation is obtained by the extraction of a small fraction A_{LO} of the incoming field A_0 by means of a beam splitter α of reflectance r_α and transmittance t_α. Successively this field is phase-modulated at high frequency ($\approx 10^7\,Hz$) by an electro-optical device and recombined with the output field A_T on the beam splitter β of reflectance r_β and transmittance t_β.

The interferring field $A = r_\beta A_{LO} + t_\beta A_T$ is detected by a photo-diode, whose output current is demodulated, filtered and finally through the lock-in technique the significative interferometer signal is extracted.

In the given hypothesis the intensities of the involved fields are quantitatively given by the inequalities :

$$|A_0|^2 >> |A_{LO}|^2 >> |A_T|^2 \tag{1}$$

The intensity $|A|^2$ hitting the photo-diode is given by the expression:

$$|A|^2 = r_\beta^2 r_\alpha^2 |A_0|^2 + t_\beta^2 |A_T|^2 + 2 r_\alpha r_\beta t_\beta |A_0| |A_T| \cos\left[\theta + m \sin(\omega_M t)\right] \tag{2}$$

where θ is the interfering field phase, m and ω_M the amplitude and the frequency of the external phase-modulation.

The phase θ can be adjusted to the value $\pi/2$ in order to express the intereference term of $|A|^2$ in odd Bessel's function series (actually limited to the fundamental frequency by means of electronic filtering) and neglecting $|A_T|^2$ the expression (2) becomes:

$$|A|^2 \simeq r_\alpha^2 r_\beta^2 |A_0|^2 - 4 r_\alpha r_\beta t_\beta |A_0| |A_T| J_1(m) \sin(\omega_M t) \tag{3}$$

The current i of a photo-diode, excited by a light of power $|A|^2$ integrated on the photo-diode surface, is given by the expression:

$$i = e\eta \frac{|A|^2}{h\nu} \tag{4}$$

where e is the electronic charge, η the quantum efficiency and $h\nu$ the photon energy. It results that the photo-diode output current is given by a "dc" component and an "ac" component of frequency $\omega_M/2\pi$.
The current signal i_s given by the lock-in technique is written as :

$$i_s = \frac{e\eta}{h\nu} 4 r_\alpha r_\beta t_\beta \left|A_0\right| \left|A_T\right| J_1 \tag{5}$$

and the noise current i_n, coming from the photo-diode shot noise relatively to the "dc" component, is given by the formula :

$$i_n = \sqrt{< i^2 >} = \sqrt{2e\Delta f \frac{e\eta}{h\nu}} r_\alpha r_\beta \left|A_0\right| \tag{6}$$

Therefore the signal to noise ratio can be written :

$$SNR = \frac{i_s}{i_n} = \sqrt{\frac{2\eta}{h\nu\Delta f}} 2 t_\beta \left|A_T\right| J_1 = \sqrt{\frac{2\eta \left|A_0\right|^2 \eta_R}{h\nu}} \sqrt{2} J_1 \sigma_{BS} \left|F\right| \frac{\Delta\Phi\left(\nu_g\right)}{\sqrt{\Delta f}} \tag{7}$$

having taken into account that $t_\beta = 1/\sqrt{2}$.

Appendix-B

According to the ref.16, the field of a resonant device can be given by means of a couple of differential equations of the first order (instead of a second order differential equation), no matter the frequency range be involved. Such a couple of differential equations gets the form :

$$\begin{aligned} \dot{A}_+ &= -\left(\frac{1}{\tau} - j\omega_0\right) A_+ + kS_+ \\ \dot{A}_- &= -\left(\frac{1}{\tau} + j\omega_0\right) A_- + kS_+^* \end{aligned} \tag{1}$$

where the *dot* means time-derivation and the *star* complex conjugation.
$A_\pm$ indicates the field into the resonator; $S_+ = S_0 \exp[j\omega t]$ is the exciting field, ω_0 the resonance circular frequency;furthermore the following definitions are given :

$$\frac{1}{\tau} = \frac{1}{\tau_e} + \frac{1}{\tau_0} \qquad \frac{1}{\bar{\tau}} = \frac{1}{\tau_e} - \frac{1}{\tau_0} \qquad k^2 = \frac{1}{\tau} + \frac{1}{\bar{\tau}} \tag{2}$$

where τ_0 is the relaxation time due to the resonator energy-losses and τ_e the relaxation time due to the energy escaping from the resonator.
Following the ref.16 notations, the field S_- reflected by the resonator is written as :

$$S_- = -S_+ + kA \tag{3}$$

where by A the fields A_+ or A_- are indicated.
The explicit expression of S_- (or S_-^*) can be obtained by using the first (or the second) equation of the system (1), being the first equation the complex conjugate of the second one :

$$S_-(t) = S_+(t)\,\Gamma\frac{1 - j\delta\bar{Q}}{1 + j\delta Q} = S_0\frac{\Gamma - j\delta Q}{1 + j\delta Q}\exp(j\omega t) \tag{4}$$

where the following definitions hold :

$$\delta = \frac{\omega - \omega_0}{\omega_0} \qquad Q = \omega_0 \tau \qquad \bar{Q} = \omega_0 \bar{\tau} \qquad \Gamma = \frac{\tau}{\bar{\tau}} \tag{5}$$

If a small harmonic perturbation $h(t) = h\cos(\Omega t)$ is supposed to affect the resonant device in such a way that neither the resonance frequency ω_0 nor the relaxation time τ be longer constant, then the time dependent expression of these parameters can be given in the form :

$$j\omega_0(t) - \frac{1}{\tau(t)} = j\omega_0 - \frac{1}{\tau} + j\Delta\omega_0(t) + \frac{\Delta\tau(t)}{\tau^2} \tag{6}$$

If the expression (6) is applied to an optical cavity of optical length d_0 and if the perturbation is responsible of a harmonic vibration $\Delta d(t)$ of the cavity optical length around the resonant value d_0 ($h = \Delta d/d_0$), then the expression (6) becomes :

$$j\omega_0(t) - \frac{1}{\tau(t)} = \left[j\omega_0 - \frac{1}{\tau}\right](1 - h\cos(\Omega t)) \tag{7}$$

remembering the following relations : $\Delta\omega_0/\omega_0 = -\Delta d/d_0$ and $\tau = F^* 2d_0/\pi c$ concerning the cavity.
The calculation leading to the expression of the reflected field $S_-(t)$ can be repeated in the case of the perturbed condition (7).
The differential equation gets the perturbed form :

$$\dot{A}(t) = -\left(\frac{1}{\tau} - j\omega_0\right)[1 - h\cos(\Omega t)]A(t) + kS_+ \tag{8}$$

The field $A(t)$ can be expanded in series of the perturbation amplitude h :

$$A(t) = A_0(t) + hA_1(t) + O(h) \tag{9}$$

by using the hypothesis of the perturbation smallness, the terms $O(h)$ can be neglected.
The expression (9) and its time derivative allow to write the equation (8) as:

$$\dot{A}_0 + \gamma A_0 - kS_+ = -h\left[\gamma\left(A_1 - A_0\cos\left(\Omega t\right)\right) + \dot{A}_1\right] \tag{10}$$

where γ is defined as : $\gamma = 1/\tau - j\omega_0$.
The equation (10) requires the fulfillment of the following system of differential equations:

$$\begin{aligned} &\dot{A}_0 + \gamma A_0 - kS_+ = 0 \\ &\dot{A}_1 + \gamma\left[A_1 - A_0\cos\left(\Omega t\right)\right] = 0 \end{aligned} \tag{11}$$

The system (11) supplies the following solution for $A_0(t)$ and $A_1(t)$:

$$\begin{aligned} A_0(t) &= \frac{\tau k S_0}{1 + j\delta Q}\exp\left(j\omega t\right) \\ A_1(t) &= \frac{\gamma\tau^2 k S_0/2}{1 + j\delta Q}\left[\frac{\exp\left(j\omega_+ t\right)}{1 + j\delta_+ Q} + \frac{\exp\left(j\omega_- t\right)}{1 + j\delta_- Q}\right] \end{aligned} \tag{12}$$

where :

$$\delta_\pm = \frac{\omega \pm \Omega - \omega_0}{\omega_0} \tag{13}$$

Therefore the expression (9) can be rewritten as:

$$A(t) = \frac{\tau k S_0}{1 + j\delta Q}\left[\exp\left(j\omega t\right) + h\frac{\gamma\tau}{2}\left(\frac{\exp\left(j\omega_+ t\right)}{1 + j\delta_+ Q} + \frac{\exp\left(j\omega_- t\right)}{1 + j\delta_- Q}\right)\right] \tag{14}$$

By using the expression (14) into the (3), the reflected field $S_-(t)$ gets the form :

$$\begin{aligned} S_-(t) = S_0\frac{1 + \Gamma}{1 + j\delta Q}\Bigg[&\frac{\Gamma - j\delta Q}{1 + \Gamma}\exp\left(j\omega t\right) + \\ &h\frac{\gamma\tau}{2}\left(\frac{\exp\left(j\omega_+ t\right)}{1 + j\delta_+ Q} + \frac{\exp\left(j\omega_- t\right)}{1 + j\delta_- Q}\right)\Bigg] \end{aligned} \tag{15}$$

In the optical cavity case the expression (15) can be simplified. In fact the energy-losses due to the escaping energy from the cavity are much larger

than the energy-losses into the optical components of the cavity, thus it results $\tau_e << \tau_0$ or $1/\tau \approx 1/\bar{\tau}$,therefore $\Gamma \approx 1$. In addition the factor $\gamma\tau = 1 - jQ \simeq -jQ$, since the parameter Q gets a large value in comparison to the unit.
By using this approximation the expression (15) gets the simplified expression :

$$S_-(t) \simeq \frac{S_0}{1+j\delta Q}\left[(1-j\delta Q)\exp(j\omega t) - hjQ\left(\frac{\exp(j\omega_+ t)}{1+j\delta_+ Q} + \frac{\exp(j\omega_- t)}{1+j\delta_- Q}\right)\right] \tag{16}$$

By comparing the expression (16) with the unperturbed field (4) it is apparent that the harmonic perturbation of frequency Ω originates the rising of two side band (SB_+ and SB_-) terms of frequency $\nu_\pm = \nu \pm \Omega/2\pi$ besides the carrier (CR) term of frequency ν :

$$S_-(t) = CR - SB_+ - SB_- \tag{17}$$

By matching the carrier frequency at the cavity resonance ν_0, one obtains the resonance conditions : $\delta = 0$ and $\delta_\pm = \pm\Omega/\omega$.
We are also interested to get the perturbed expression of the transmitted intensity relatively to the resonator connected to two guides.
In fact such a structure is quite similar to the optical configuration used in the narrow band version of the interferometric antenna.
In this case the equation corresponding to the first equation of the system (1) of the previous calculation is:

$$\dot{A} = -(1/\tau - j\omega_0)A + k_1 S_{+1} + k_2 S_{+2} \tag{18}$$

where the relaxation time τ and the coupling factor k_μ are defined as:

$$\frac{1}{\tau} = \frac{1}{\tau_0} + \frac{1}{\tau_{e1}} + \frac{1}{\tau_{e2}} \qquad k_\mu^2 = \frac{2}{\tau_{e\mu}} \tag{19}$$

being τ_0 the relaxation time of the resonator and $\tau_{e\mu}$ the relaxation time due to the energy escaping from the $\mu - th$ guide.
Besides the field $S_{+\mu}$ indicates the field exciting the resonator coming from the $\mu - th$ guide ($\mu = 1, 2$).
The reflected wave $S_{-\mu}$ is evaluated using a generalization of (3):

$$S_{-\mu} = -S_{+\mu} + k_\mu A \tag{20}$$

The field transmitted by the resonator can be expressed by the field exchanged by two guides; hence, substituting the (20) into (18), the transmitted field S_{-2} becomes:

$$S_{-2} = k_2 A = S_{+1} \frac{2\tau/\sqrt{\tau_{e1}\tau_{e2}}}{1 + j(\omega - \omega_0)\tau} \tag{21}$$

the transmitted intensity is given by the expression:

$$|S_{-2}|^2 = |S_{+1}|^2 \frac{4\tau^2/(\tau_{e1}\tau_{e2})}{1 + (\omega - \omega_0)^2\tau^2} \tag{22}$$

The field transmitted by the resonator, if a harmonic perturbation is present in the system, is easily obtained by substituting the perturbed field (14) into (21), adding to parameters k and τ the lower index indicating that the guide 2 is considered:

$$S_{-2} = \frac{\tau_2 k_2^2 S_0}{1 + j\delta Q} \left[\exp(j\omega t) + h\frac{\gamma\tau_2}{2} \left(\frac{\exp(j\omega_+ t)}{1 + j\delta_+ Q} + \frac{\exp(j\omega_- t)}{1 + j\delta_- Q} \right) \right] \tag{23}$$

the comparison of definition (2) and (19) supplies the relation between the relaxation times τ and τ_2: $\tau_2 = 2\tau$.

Appendix-C

Since the optical system of an interferometric antenna is rather a complex one, as it is apparent throughout this paper, it is not unusual, in discussing about the antenna behaviour, to be confused in considering partial characteristics of the optical system as characteristics of the antenna itself or in estimating the phase sensitivity without performing an accurate analysis of the phase perturbation the antenna is subjected.
For these reasons we feel it is useful to discuss in details the *global* characteristics of the antenna optical system, i.e. in considering this system as a *black box* and studying its *response* if subjected to some typical phase perturbation.
The optical system we study is a Michelson interferometer having optical cavities as reflecting elements in its arms and a front reflector (recycling mirror) in order to send back the interferometer energy flux.
We call this optical system *resonant* if the following four conditions are fulfilled :

i) The interferometer arm cavities are resonant at laser frequency ν_0 :

$$\exp\left(i2\pi\nu_0\frac{2d_0}{c}\right) = -\left[\exp\left(i2\pi\Delta\nu\frac{2d_0}{c}\right)\right]_{\Delta\nu=0} = -1 \tag{1}$$

ii) The optical length difference $l_2 - l_1$ gives the Michelson extinction condition :

$$\exp\left(i2\pi\nu_0 2\frac{l_2 - l_1}{c}\right) = -\left[\exp\left(i\pi\frac{\Delta\nu}{\nu_0}\right)\right]_{\Delta\nu=0} = -1 \tag{2}$$

iii) The optical lengths $l + l_1$ and $l + l_2$ of the recycling cavities are resonant at laser frequency ν_0 :

$$\exp\left(i2\pi\nu_0\frac{l + l_{1,2}}{c}\right) = \left[\exp\left(i2\pi\frac{\Delta\nu}{\nu_0}\right)\right]_{\Delta\nu=0} = 1 \tag{3}$$

iv) The recycling mirror reflectance ρ gets one suitable value in order to vanish the back field :

$$\rho = \sigma_R \sigma_{BS} |F| \tag{4}$$

where in all used expressions the symbols have been already defined in the text (see also Fig.2).

If we consider the perturbation, the gravitational antenna has been designed for, i.e. opposite length variations of the interferometer arm optical cavities, only the condition i) is violated.
We point out that in this case the fields reflected by the FP cavities supply the information of the length variation through their phases and no through their amplitudes. That because their amplitude is almost unitary ($|F| \simeq 1$). In other words the FP cavities behave as *phase objects*[14].
On the contrary, if we look at the *response* of the optical system in the case the perturbation be due to the laser frequency variation $\Delta\nu$ around the resonant frequency ν_0, we observe that the conditions i),ii) and iii) are not fulfilled. Therefore the optical system behaviour will be completely different from the previous one.
In the following we report calculations of the optical system response in these two mentioned typical cases of phase perturbation in order to focus the involved differences.
That is done by calculating the transmitted and reflected intensity of the optical system and studying the phase dependence in order to explor the involved time constants of the system.
First we consider the case where the optical system is *resonant* and the phase perturbation is due to the opposite length variations of the Michelson arm cavities.
By using the formulae (7) and (14) of the text we calculate the transmitted intensity taking into account that the following relations hold between the complex reflectances F_μ ($\mu = 1, 2$) of the FP's cavities :

$$F_{1,2} = |F| \exp\left[i(\pi \pm \arctan\left(\frac{(\alpha+\beta)\tan\Delta\delta/2}{1-\alpha\beta\tan^2\Delta\delta/2}\right))\right] \simeq \tag{5}$$
$$\simeq -|F| \exp\left[\pm i \arctan\left(\frac{2(2\Delta\nu/\nu_{FP})}{1-(2\Delta\nu/\nu_{FP})^2}\right)\right]$$

being :

$$|F|^2 = \frac{(\frac{\sigma r_2 - r_1}{1 - r_1 r_2})^2 + \sigma(\frac{2\Delta\nu}{\nu_{FP}})^2}{1 + (\frac{2\Delta\nu}{\nu_{FP}})^2} \simeq 1 \tag{6}$$

in the approximations $r_1^2 < r_2^2 \simeq \sigma \simeq 1$ and $\sin(\Delta\delta/2) \simeq \Delta\delta/2$ (remember the formulas (18) of text defining α and β).
By the symbol ν_{FP} the FP cavity width is indicated, defined as the *free spectral range* divided by the *finesse* F^* ($\nu_{FP} = c/2d_0F^*$).
By using the formula (7) of text in calculating the transmitted intensity and having taken into account the conditions i),ii),iii) and iv) in the $F_{1,2}$ expression given by (17), one obtains the result :

$$\begin{aligned}
\left|\frac{A_T}{A_{IN}}\right|^2 &= \sigma_{BS}^2 |F|^2 \left[\frac{2(\sqrt{\eta_R}\, 2\Delta\nu/\nu_{FP})}{1 + \frac{1+\sigma_R\sigma_{BS}^2|F|^2}{\sigma_R}(\sqrt{\eta_R}\, 2\Delta\nu/\nu_{FP})^2}\right]^2 \simeq \\
&\simeq 2\left[\frac{(\sqrt{2\eta_R}\, 2\Delta\nu/\nu_{FP})}{1 + (\sqrt{2\eta_R}\, 2\Delta\nu/\nu_{FP})^2}\right]^2 = \\
&= \frac{1}{2}\sin^2\left[2\arctan\left(\sqrt{2\eta_R}\, 2\Delta\nu/\nu_{FP}\right)\right]
\end{aligned} \tag{7}$$

and for the reflected intensity one obtains :

$$\left|\frac{A_R}{A_{IN}}\right|^2 = \frac{1}{2}\left(\sqrt{2\eta_R}\frac{2\Delta\nu}{\nu_{FP}}\right)^2 \left|\frac{A_T}{A_{IN}}\right|^2 \tag{8}$$

where the approximation $\sigma_R\sigma_{BS}^2 |F|^2 \simeq 1$ has been done and having put the transmitted intensity in the form of squared sinus of the argument $2\arctan(\sqrt{2\eta_R}\, 2\Delta\nu/\nu_{FP})$.
That gives the functional character of the transmitted and reflected intensity versus the argument $\sqrt{2\eta_R}2\Delta\nu/\nu_{FP}$ (see Fig. 7).
It is important to discuss the form of the field reflected by the FP cavity in the case of a harmonic perturbation of frequency $\Omega/2\pi$ of the cavity length around the resonant length d_0 ($d = d_0 + \Delta d \sin\Omega t$); in general we have :

$$\begin{aligned}
&a(t) = a_0 \exp\left[i\omega_0 t - i\Phi\sin\Omega t\right] \simeq \\
&a_0 \exp\left(i\omega_0 t\right)[1 - i\Phi\sin\Omega t] \simeq
\end{aligned}$$

$$a_0 \exp(i\omega_0 t)[1 - \frac{\Phi}{2}(\exp(i\Omega t) - \exp(-i\Omega t))] =$$
$$a_0[\exp(i\omega_0 t) + \frac{\Phi}{2}\exp(i\omega_+ t) - \frac{\Phi}{2}\exp(-i\omega_- t)] \tag{9}$$

where the circular frequencies $\omega_\pm$ are defined as :

$$\omega_\pm = \omega_0 \pm \Omega \tag{10}$$

the (9) tells to us that a harmonic perturbation produces side bands at circular frequencies ω_+ and ω_-, thus the phase amplitude Φ can be evaluated as :

$$\Phi = \frac{\left|a_0 \frac{\Phi}{2}\exp(i\omega_+ t)\right| + \left|a_0 \frac{\Phi}{2}\exp(-i\omega_- t)\right|}{|a_0 \exp(-i\omega_0 t)|} \tag{11}$$

From (11) (see the calculation of Appendix-B) one obtains the formula (44) of text :

$$\Delta\Phi(\Omega) = 2\frac{\Delta d}{d_0}\frac{\omega_0 \tau}{\sqrt{1+\Omega^2\tau^2}} \tag{12}$$

where $\tau = 1/\pi\nu_{FP}$ (see formula (42) of text).
The result (12) can be put into (7) performing the following reasonable approximation of the phase : $\Delta\Phi \simeq -4\Delta\nu/\nu_{FP}$. One obtains the expression :

$$\left|\frac{A_T}{A_{IN}}\right|^2 = \frac{1}{2}\sin^2[2\arctan(\sqrt{2\eta_R}\,\Delta\Phi(\Omega)/2)] =$$
$$\frac{1}{2}\sin^2[2\arctan(\sqrt{2\eta_R}\,\frac{\Delta d}{d_0}\frac{\omega_0\tau}{\sqrt{1+\Omega^2\tau^2}})] \tag{13}$$

in the case of GW detection $\Delta d/d_0$ is given by the strain of the wave and it is a very small quantity, therefore in practice the (13) becomes :

$$\left|\frac{A_T}{A_{IN}}\right|^2 \simeq 4\eta_R\frac{\omega_0^2\tau^2}{1+\Omega^2\tau^2}(\frac{\Delta d}{d_0})^2 \tag{14}$$

however, as shown in the text, we are able to look at squared root of (14), linear in the perturbation amplitude, by means of the modulation technique (see the formula (45) of text) .
The time constant τ appearing into (14), which characterizes the time response of the interferometric antenna, is actually depending only on the FP cavity width and just it determines the frequency cut reducing to one half the transmitted intensity ($\Omega\tau = 1$).
The time constants characteristic of other parts of the interferometer don't play any role in GW detection.
This fact is understandable for several reasons.
First in this type of perturbation only the long cavities are excited and the other parts of the system remain in the resonant state.
Second, in the GW detection case, the FP cavity perturbation is so small that the ΔQ variation involved is of the order of 10^{-19}, therefore the relative change in the stored energy is extremely small. That makes sure that the cavity behaves really as a *phase object.*
It can be also proved that under this type of phase perturbation the energy stored into the recycling cavities is subjected to a percentage variation as small as the long arm cavities.
In order to compare this case with the case where the phase perturbation is generated by a laser frequency variation around the resonance frequency ν_0, we report in the following the calculation of the transmitted and reflected intensity of the optical system as function of the detuning $\Delta\nu$.
This case is characterized by the fact that the conditions i),ii),and iii) are violated at same time and that the phase variations into the FP cavities are equal :

$$F_1 = F_2 = |F| \exp(i\phi) = |F| \exp\left[i(\pi + \arctan\left(\frac{2(2\Delta\nu/\nu_{FP})}{1-(2\Delta\nu/\nu_{FP})^2}\right))\right] =$$
$$|F| \exp\left[i(\pi + \arctan\left(\frac{2px}{1-(px)^2}\right))\right] \tag{15}$$

where by definition is settled :

$$x = \frac{\Delta\nu}{\nu_0} \qquad p = \frac{2\nu_0}{\nu_{FP}} \qquad px = \frac{2\Delta\nu}{\nu_{FP}} \tag{16}$$

Starting from the formulae (6) and (7) of text we obtain the expressions of the reflected and transmitted intensities :

$$\left|\frac{A_R}{A_{IN}}\right|^2 = \frac{\rho^2[1+\cos^2(\frac{\pi}{2}x)+2\cos(\phi+\frac{5}{2}\pi x)\cos(\frac{\pi}{2}x)]}{1+(\rho^2/\sigma_R)^2\cos^2(\frac{\pi}{2}x)+2(\rho^2/\sigma_R)\cos(\phi+\frac{5}{2}\pi x)\cos(\frac{\pi}{2}x)} \quad (17)$$

$$\left|\frac{A_T}{A_{IN}}\right|^2 = \frac{[\rho^2(\sigma_R-\rho^2)/\sigma_R]\sin^2(\frac{\pi}{2}x)}{1+(\rho^2/\sigma_R)^2\cos^2(\frac{\pi}{2}x)+2(\rho^2/\sigma_R)\cos(\phi+\frac{5}{2}\pi x)\cos(\frac{\pi}{2}x)} \quad (18)$$

where the value of ρ^2 is fixed by the condition iv).
In discussing the (17) and (18) it is convenient to evaluate them in two separated ranges of x parameter :

$$0 \leq x < 10^{-2} \qquad 10^{-2} \leq x \leq 1 \quad (19)$$

because in two cases the (17) and (18) can be approximated in different way. In fact in the first range it is legal the sinus, cosinus series expansion neglecting powers larger than the second one.
Thus, in studying first the reflected intensity expression (17) for the former range, the term $\cos(\phi+\frac{5}{2}\pi x)\cos(\frac{\pi}{2}x)$ can be approximated as :

$$\cos(\phi+\frac{5}{2}\pi x)\cos(\frac{\pi}{2}x) \simeq (1-13(\frac{\pi}{2}x)^2)\cos\phi - \frac{5}{2}\pi x\sin\phi \quad (20)$$

and the (17) gets the expression :

$$\left|\frac{A_R}{A_{IN}}\right|^2 = \frac{\rho^2[2-(\frac{\pi}{2}x)^2+2((1-13(\frac{\pi}{2}x)^2)\cos\phi-\frac{5}{2}\pi x\sin\phi)]}{1+(\frac{\rho^2}{\sigma_R})^2(1-(\frac{\pi}{2}x)^2)+\frac{2\rho^2}{\sigma_R}[(1-13(\frac{\pi}{2}x)^2)\cos\phi-\frac{5}{2}\pi x\sin\phi]} \quad (21)$$

recalling the ϕ definition (15) the $\cos\phi$, $\sin\phi$ expressions become :

$$\cos(\phi) = -\frac{1-(px)^2}{1+(px)^2} \qquad \sin(\phi) = -\frac{2(px)}{1+(px)^2} \quad (22)$$

By substituting the (22) into (21) one obtains :

$$\left|\frac{A_R}{A_{IN}}\right|^2 = \frac{\rho^2[4(px)^2 + 5\pi x(px) + 25(\frac{\pi}{2}x)^2]}{(1-\frac{\rho^2}{\sigma_R})^2 + (1+\frac{\rho^2}{\sigma_R})^2(px)^2 + [10\pi x(px) + (26-\frac{\rho^2}{\sigma_R})(\frac{\pi}{2}x)^2]\frac{\rho^2}{\sigma_R}} =$$

$$= \frac{\rho^2[4 + (\frac{5\pi}{2p})^2 + \frac{5\pi}{p}]x^2}{(\frac{1-\rho^2/\sigma_R}{p})^2 + x^2[(1+\frac{\rho^2}{\sigma_R})^2 + \frac{\rho^2}{\sigma_R}(\frac{\pi}{2p})^2(26-\frac{\rho^2}{\sigma_R}) + 10\pi\frac{\rho^2}{p\sigma_R}]} \simeq$$

$$\simeq \left(\frac{2\rho\sigma_R}{\sigma_R+\rho^2}\right)^2 \frac{x^2}{\left(\frac{\sigma_R-\rho^2}{\sigma_R+\rho^2}\right)^2/p^2 + x^2} \tag{23}$$

having neglected into the brakets of (23) the terms divided by p, being p a very large quantity ($p \approx 10^{11}$).
Recalling the condition iv), one realizes that $\rho/\sqrt{\sigma_R}$ is a quantity very close to unit; therefore expressing $\rho/\sqrt{\sigma_R} = 1 - \varepsilon$, where $\varepsilon << 1$, and neglecting terms $O(\varepsilon)$ the following factors appearing into (22) can be written as :

$$\left(\frac{2\rho\sigma_R}{\sigma_R+\rho^2}\right)^2 \simeq \sigma_R \approx 1 \qquad \left(\frac{\sigma_R-\rho^2}{\sigma_R+\rho^2}\right) \approx \varepsilon \tag{24}$$

thus the (22) becomes :

$$\left|\frac{A_R}{A_{IN}}\right|^2 \simeq \frac{\sigma_R x^2}{(\varepsilon/p)^2 + x^2} \tag{25}$$

The functional behaviour of (25) is very clear : it gets the value $\sigma_R \approx 1$ for $x > \varepsilon/p \approx 10^{-13}$ and goes to zero limit as x^2; in particular it reaches the value $1/2$ for $x_{1/2} = \varepsilon/p$.
Recalling the p definition (16), one can calculate the optical system width FWHM as $\Delta\nu_{FWHM} = \nu_0 2\varepsilon/p$.
We point out that $\Delta\nu_{FWHM}$ gets a noticeable expression by using the ε, p and the recycling factor η_R definitions :

$$\Delta\nu_{FWHM} = 2\nu_0\frac{1-\rho/\sqrt{\sigma_R}}{2\nu_0}\nu_{FP} = \frac{\sigma_R-\rho^2}{\sigma_R+\rho^2}\nu_{FP} \simeq \frac{\nu_{FP}}{2\eta_R} \tag{26}$$

the (26) shows that the optical system width is given by the FP cavity width reduced by the recycling factor.
Besides the corresponding relaxation time $2\eta_R F^* 2d_0/c$ can be compared with the relaxation time coming from the Q-value of the resonant system. Following the VIRGO project numbers (see in section 4 the iii) calculation data), it results :

$$Q = 2\pi\nu_0 \frac{2.7\,Joule}{10\,Watt} = .27\omega_0 = \omega_0\tau \qquad or \qquad \tau = .27\,sec \tag{27}$$

by using the same numerical values of iii) in evaluating the relaxation time coming from (26), one obtains $\tau = .42\,sec$ in reasonable agreement with (27).
As far as the transmitted intensity (18) is concerned, by using the same approximations, one gets the following expression :

$$\left|\frac{A_T}{A_{IN}}\right|^2 \simeq \frac{\rho^2}{\sigma_R}(1-\frac{\rho^2}{\sigma_R})(\frac{\pi}{2p})^2 \frac{x^2}{\left(\frac{\sigma_R-\rho^2}{\sigma_R+\rho^2}\right)^2/p^2 + x^2} \tag{28}$$

which shows a functional behaviour as (23), but tremendously suppressed by the factor $1/p^2 \approx 10^{-22}$.
In the case of the latter x range (19) we point out that with excellent approximation the following inequality holds :

$$\left|\arctan\left(\frac{2px}{1-(px)^2}\right)\right| \simeq \left|-\arctan\left(\frac{2}{px}\right)\right| \simeq \frac{2}{px} << \frac{5}{2}\pi x \tag{29}$$

therefore the (17) can be written as :

$$\left|\frac{A_R}{A_{IN}}\right|^2 = \frac{\rho^2[1+\cos^2(\frac{\pi}{2}x) - 2\cos(\frac{5}{2}\pi x)\cos(\frac{\pi}{2}x)]}{1+(\rho^2/\sigma_R)^2\cos^2(\frac{\pi}{2}x) - 2(\rho^2/\sigma_R)\cos(\frac{5}{2}\pi x)\cos(\frac{\pi}{2}x)} \tag{30}$$

By putting into (30) the following typical numerical values :

$$\sigma_R = .9999 \qquad \sigma_{BS} = .999 \qquad \rho^2 = (\sigma_R\sigma_{BS}\,|F|)^2 = .9938 \tag{31}$$

we deduce that $\rho^4/\sigma_R^2 = .987864$ and $2\rho^2/\sigma_R = 1.987827$.
The equality of the first four decimal digits of these factors makes sure that the behaviour of (30) versus x begins to fall for x values smaller than 10^{-4}, therefore the (30) holds the value ρ^2 in the whole range ($10^{-2} \leftrightarrow 1$) and it matches correctly the value of the former case.
The transmitted intensity in the latter range (19) gets the expression :

$$\left|\frac{A_T}{A_{IN}}\right|^2 = \frac{(\rho/\sigma_R)^2(\sigma_R - \rho^2)\sin^2\left(\frac{\pi}{2}x\right)}{1 + (\rho^2/\sigma_R)^2\cos^2\left(\frac{\pi}{2}x\right) - 2(\rho^2/\sigma_R)\cos\left(\frac{5}{2}\pi x\right)\cos\left(\frac{\pi}{2}x\right)} \tag{32}$$

the (32) exhibits a gentle rising in the x region ($10^{-2} \leftrightarrow .5$) up to value $\sim .2(\sigma_R - \rho^2)$ (note that $\sigma_R - \rho^2 \approx 10^{-2}$), then rises quickly crossing $\sigma_R - \rho^2$ at $x = .66$ and reaches its maximum value $2(\sigma_R - \rho^2)$ at $x = .77$; at last it decreases to $\sigma_R - \rho^2$ value in the $x \to 1$ limit.

Appendix-D

In this Appendix the symmetric system of three coupled optical cavities is studied.

The coupling study of resonant cavities started in the early 1944, when Bethe[24] presented a solution to the field problem of coupling two identical microwave cavities through a small circular aperture in a common conducting plane of zero thickness.

A nice experimentation of this method was made later by Melissinos et al.[25] (1985) on two superconducting coupled microwave cavities (two connected cilinders $4\,cm$ long and $4\,cm$ in diameter).

The authors were able of detecting the displacement amplitude of a harmonic perturbation of one cavity end wall as small as $3.\,10^{-19}\,m/\sqrt{Hz}$.

That demonstrates the powerfull of such method in detecting very small harmonic displacement by using the multiresonant modes of coupled cavities.

In the following the system, consisting of two equal optical cavities d_0 long connected by a short optical cavity of length a ($a << d_0$), is studied.

The end mirrors of the long cavities have very high reflectivity ($r_2^2 \simeq 1$) and the front mirrors a lower reflectivity, furthermore the energy losses into the optical elements will be considered negligible.

The entry point of the optical system is given by the recycling mirror bending the short cavity in the middle (see Fig. 5a).

As it will be shown in the following, this coupled cavities system exhibits two resonant modes and therefore it is comparable to a linear system of two equal cavities d_0 long, coupled by a common mirror of reflectivity r_x^2 (see Fig. 5d).

It can be shown that, by applying S-matrix method to three mirrors ($r_1^2 = r_2^2 \equiv r^2 \simeq 1$), this optical system gets two resonant modes at circular frequencies ω_+ and ω_- given by the expression :

$$\omega_\pm = \omega_0 \pm \frac{c}{d_0} K(r_x) \tag{1}$$

the two frequencies are located symmetrically around the resonance frequency $\omega_0 = \pi c/d_0(q + 1/2)$ and shifted by $K(r_x)c/d_0$, where $K(r_x)$ is the coupling factor of the two cavities depending on the reflectance r_x as given by the

following formula :

$$K(r_x) \simeq \arctan\left(\sqrt{\frac{1-r_x}{1+r_x}}\right) \tag{2}$$

The (2) shows that the maximim coupling is reached for $r_x \to 0$, and the resonances go to limit $\omega_0 \pm \pi c/4d_0$; on the other hand the minimum coupling is reached for $r_x^2 = 1$, when the two cavities are completely decoupled and therefore each one gets the single resonance ω_0.
Going back to three coupled cavities under study, the short cavity plays the same role as the common mirror does to two cavities of the previous case. The only difference consists that this times the coupling factor depends on two parameters : on the reflectivity r_1^2 and also on the short cavity length. As described in the text, the three cavities system is excited by two fields $A_{0\mu}$ ($\mu = 1,2$), given by the expressions (46), and four fields $A_{T\mu}$ and $A_{R\mu}$ are obtained back, whose expressions are given by (47) and (48) of the text. In the hypothesis that the energy flux neither escapes through the FP cavities ($|F| = 1$) nor is lost into the optical components ($\rho^2 + \tau^2 = 1$), the energy conservation leads to the equation:

$$|A_{0\mu}|^2 = |A_{T\mu}|^2 + |A_{R\mu}|^2 \tag{3}$$

Our aim is to calculate the resonant modes of the coupled cavity system. Hence by detuning the laser frequency around the resonance frequency ν_0 of the FP cavity, the F_μ expression ($\mu = 1,2$) becomes:

$$F_1 = F_2 = |F|\exp(Arg[F]) = \frac{\sigma r_2 - r_1}{1 - r_1 r_2}\sqrt{\frac{1+(\alpha^2-1)\sin^2(\Phi-\Phi_0)/2}{1+(\beta^2-1)\sin^2(\Phi-\Phi_0)/2}} *$$
$$\exp\left(i[\pi + \arctan(\frac{(\alpha+\beta)\tan(\Phi-\Phi_0)/2}{1-\alpha\beta\tan^2(\Phi-\Phi_0)/2})]\right) \simeq$$
$$\exp\left(i[\pi + \arctan(\frac{2q\tan(\Phi-\Phi_0)/2}{1-q^2\tan^2(\Phi-\Phi_0)/2})]\right) \tag{4}$$

having used the following definitions:

$$\Phi - \Phi_0 = \frac{2d_0}{c}(\omega - \omega_0) \qquad\qquad q = \frac{1 + r_1}{1 - r_1} \tag{5}$$

By substituting the expression (4) into the equation (3), one verifies that it is identically fulfilled for any value of the cosinus argument:

$$\frac{\tau^4 + 2\rho^2[1 - \cos 2(ka + Arg[F])]}{(1 - \rho^2)^2 + 2\rho^2[1 - \cos 2(ka + Arg[F])]} = 1 \tag{6}$$

therefore it is allowed to write:

$$2Arg[F] + 2ka = \gamma 2\pi \qquad mod(2\pi) \tag{7}$$

where γ is a parameter defined in the range $(0 \leftrightarrow 1)$.
For simplicity sake we rewrite (7) in the form:

$$Arg[F] = \psi \qquad \psi = \gamma\pi - ka \tag{8}$$

and by using the expression (4), we have:

$$\pi + \arctan\left(\frac{2q\tan(\Phi - \Phi_0)/2}{1 - q^2\tan^2(\Phi - \Phi_0)/2}\right) = \psi \tag{9}$$

the (9) leads to a second order algebric equation in the variable $\tan(\Phi - \Phi_0)/2$, which gives the following solution:

$$\begin{aligned} \Phi_1 &= \Phi_0 - 2\arctan\left(\frac{\cot\psi/2}{q}\right) \\ \Phi_2 &= \Phi_0 + 2\arctan\left(\frac{\tan\psi/2}{q}\right) \end{aligned} \tag{10}$$

The (10) gets a general validity, however, since we want to detect the antenna response on the transmitting beam, we impose the condition $|A_{\mu T}|^2 = 1$ ($|A_{\mu R}|^2 = 0$), which is fulfilled for $\gamma = 1$.

Hence the solution (10) becomes:

$$\Phi_1 = \Phi_0 + 2\arctan\left(\frac{\cot\phi/4}{q}\right)$$
$$\Phi_2 = \Phi_0 - 2\arctan\left(\frac{\tan\phi/4}{q}\right) \tag{11}$$

having defined $\phi = 2ka$.
From (11) the circular frequencies of the optical system resonant modes can be easily obtained:

$$\omega_+ = \omega_0 + \frac{c}{d_0}\arctan\left(\frac{\cot\phi/4}{q}\right)$$
$$\omega_- = \omega_0 - \frac{c}{d_0}\arctan\left(\frac{\tan\phi/4}{q}\right) \tag{12}$$

as it is apparent from the (12) the two frequencies are located around the frequency ω_0, which is, of course, the resonance frequency of a single optical cavity d_0 long. The symmetric configuration around ω_0 is reached for $\phi = \pi$.
It is interesting to investigate about the character of the fields into the cavities, when they are excited on the frequency ω_+ or ω_-.
It will be demonstrated in the following that the case of the ω_+ (ω_-) excitation corresponds to the symmetric (antisymmetric) configuration of the fields inside the long cavities.
We consider in general two cavities and we suppose the field $a_\mu(t)$ be present inside the $\mu - th$ cavity d_μ long ($\mu = 1, 2$), having the resonance frequency $\omega_\mu = (q + 1/2)\pi c/d_\mu$.
In the coupled configuration the fields obey to the following system of differential equations :

$$\dot{a}_1(t) = j\omega_1 a_1(t) + K_{12}a_2(t)$$
$$\dot{a}_2(t) = j\omega_2 a_2(t) + K_{21}a_1(t) \tag{13}$$

where K_{12} and K_{21} are the coupling factors.
In the hypothesis of requiring for the system (13) the harmonic solution

$a_\mu(t) = a_{0\mu} \exp(j\omega t)$, by using the necessary condition that the determinant of (13) be vanishing, the following solution can be obtained :

$$\omega_\pm = \frac{\omega_1 + \omega_2}{2} \pm \sqrt{(\frac{\omega_1 - \omega_2}{2})^2 + |K_{12}|^2} \tag{14}$$

having taken into account that the coupling factors are tied by the relation[16]: $K_{12} + K_{21}^* = 0$.
In particular the (14) gives the formula (1) if $\omega_1 = \omega_2$.
Putting the solution (14) into the (13) the following equation system can be written :

$$\begin{aligned} a_{01} j\omega_\pm - j\omega_1 a_{01} - K_{12} a_{02} &= 0 \\ a_{02} j\omega_\pm - j\omega_2 a_{02} - K_{21} a_{01} &= 0 \end{aligned} \tag{15}$$

which implies that the coupling factors are pure imaginary quantities : $K_{12} = j\,|K_{12}|$ and $K_{21} = j\,|K_{21}|$.
It is straightforward to deduce from both equations of the system (15) the following relations between the fields a_{01} and a_{02}:

$$\begin{aligned} \frac{a_{02}}{a_{01}} &= \frac{1}{K_{12}} \left[\frac{\omega_1 - \omega_2}{2} \pm \sqrt{(\frac{\omega_1 - \omega_2}{2})^2 + |K_{12}|^2} \right] \\ \frac{a_{01}}{a_{02}} &= \frac{1}{K_{21}} \left[\frac{\omega_2 - \omega_1}{2} \pm \sqrt{(\frac{\omega_1 - \omega_2}{2})^2 + |K_{21}|^2} \right] \end{aligned} \tag{16}$$

the (16) for $\omega_1 = \omega_2$ leads to the common result : $a_{01}/a_{02} = \pm 1$ in the rigorous correspondence to the solutions ω_+ and ω_-.
By extending this result to the coupled cavities under study, it results that the excitation of the ω_+ (ω_-) resonances produces symmetric (antisymmetric) field configuration in the long cavities.
Therefore it is convenient to rename the resonance frequency labels indicating the corresponding field character; i.e.:

$$\omega_+ \equiv \omega_S \qquad\qquad \omega_- \equiv \omega_A \tag{17}$$

The difference of two circular frequencies (12) gets the expression:

$$\omega_S - \omega_A = \frac{c}{d_0}\left(\arctan\left[\frac{\tan(\phi/4)}{q}\right] + \arctan\left[\frac{\cot(\phi/4)}{q}\right]\right) =$$
$$\frac{c}{d_0}\arctan\left[\frac{1-r_1^2}{2r_1\sin(\phi/2)}\right] \tag{18}$$

As it is shown in the text, the difference (18) allows the tuning of the antenna, hence it is important to investigate its functional dependence on the involved parameters r_1 and ϕ.
Since r_1 is not an easy variable parameter, the variation of (18) can be achieved through the phase $\phi = k2a$ (see Fig. 8).
In fact for $\phi = 0, 2\pi$ the (18) gives $\omega_S - \omega_A = \pi c/2d_0$, which is the maximum difference reachable and it corresponds to the maximum coupling between the two long cavities.
On the contrary $\phi = \pi$ gives $\omega_S - \omega_A = \arctan[(1-r_1^2)/2r_1]c/d_0$, which is the minimum difference reachable and it corresponds to the minimum coupling between the long cavities.
In the rough approximation $r_1 \approx 1$ the maximum and minimum frequency difference results :

$$\phi = 0, 2\pi \qquad \nu_S - \nu_A = \frac{c}{4d_0} \tag{19}$$

$$\phi = \pi \qquad \nu_S - \nu_A \simeq \frac{1}{\pi}\frac{c}{2d_0}(1-r_1) \simeq \frac{1}{\pi\tau} \tag{20}$$

ACKNOWLEDGMENTS

It is a pleasure to thank the Prof. E.Polacco for his critical reading of the manuscript and many fruitful discussions. In particular we grateful acknowledge his suggestions and efforts in compelling us to write the Appendix-C.

One of us (V.M.) is grateful to INFN Section for the six years period of hospitality in Pisa as scientific collaborator and also thanks warmly the VIRGO group people for the friendly time spent together and the fruitful scientific collaboration.

REFERENCES

1) - R.Weiss, Quarterly Progress Report M.I.T. 105 (1972),54

2) - W.Winkler, Intern. Meeting on Exp. Gravitation, Pavia (1976)

3) - R.L.Foward, Phys.Rev.D Vol.17,2 (1978), 379

4) - D.Shoemaker,R.Shilling,L.Schnupp,W.Winkler,M,Maishberger, A.Rudiger, Phys.Rev.D Vol.38,2 (1988), 423

5) - R.E.Vogt (Project director) Ligo Project, M.I.T. (1989)

6) - R.W.P.Drever Gravitational Radiation, Deruelle,Pirani editors, North Holland 1983, pp.321

7) - K.A.Strain, B.J.Meers Phys.Rev.Lett. Vol.66, 11(1991),1391
B.J.Meers Phys.Rev.D Vol.38, 8 (1988),2317

8) - J.Y.Vinet,B.Meers,C.N.Man,A.Brillet
Phys.Rev.D Vol.38, 2 (1988), 433

9) - J.Y.Vinet J. Physique 47 (1986), 639
Phys. Rev.D 38,433 (1988)

10) - P.Fortini,A.Ortolani Problems of Fundamental Modern Physics, II Proc. 5th Winter School on Hadronic Physics
World Scientific 1990, editors: R.Cherubini,P.Dalpiaz,B.Minetti

11) - VIRGO Project : Final conceptual Design, Pisa (1992)

12) - C.Bradaschia,E.Calloni,M.Cobal,R.Del Fabbro,L.Di Fiore, A.Di Virgilio,A.Giazotto,L.Holloway,H.Kautzky,V.Montelatici, D.Passuello,W.Velloso INFN PI/AE 9019 (1990)

13) - P.Fortini,A.Ortolani
Nuovo Cimento,Note Brevi, Vol.106 B N.1 (1991),101.

14) - M.Born,E.Wolf, Principles of Optics Pergamon Press (1983)

15) - E.Hetch, Optics Addison-Wesly (1987)

16) - H.A.Hauss, Waves and Fields in Opto-Electronics, Prentice-Hall (1984)

17) - G.D.Boyd,J.P.Gordon, Bell Syst. Tech. Jour. (1961), 489

18) - A.E.Siegman, Lasers Univ. Science Books (1986)

19) - A.Kastler Applied Optics Vol.1 (1962),17

20) - C.W.Misner,K.S.Thorne,J.A.Wheeler, Gravitation Freeman and Company (1973)

21) - D.Fattaccioli,A.Boulharts,A.Brillet,C.N.Man, J.Optics (Paris) Vol.17, 3 (1986), 115

22) - C.N.Man,D.Shoemaker,M.Pham To,D.Dewey, Phys.Lett. A, Vol.148, 1,2 (1990), 8

23) - A.Yariv, Introduction to Optical Electronics Holt,Rinehart and Winston (1976)

24) - H.A.Bethe Phy.Rev. 966 (1944),163

25) - C.E.Reece,P.J.Reiner, A.C.Melissinos,
Nucl.Ist.Meth. in Physics Res. A245 (1986),299

26) - G.Rempe,R.J.Thompson,H.J.Kimble,R.Lalezari,
Optics Lett. Vol.17, 5 (1992), 363

FIGURE CAPTIONS

Fig. 1 - a) Optical diagram of Michelson interferometer. b) Michelson interferometer equipped with recycling mirror. c) Reflecting optical element showing the incoming and outcoming fields as used in the S-matrix technique. d) Field propagation between two reflecting optical elements.

Fig. 2 - a) Diagram of Michelson interferometer equipped with recycling mirror and resonant FP cavities at its arm ends, showing the detailed field propagation. b) Diagram showing the optical structure of the FP resonator.

Fig. 3 - Diagram of Michelson interferometer equipped with recycling mirror and resonant FP cavities, showing the external modulation and detection scheme.

Fig. 4 - Curves of the function $S(\nu_g^0)/\nu_0$ versus the GW frequency relatively to an interferometric antenna with and without recycling in the broad band case (see TABLE I for notations).

Fig. 5 - a) Optical diagram of the interferometric antenna in the narrow band version. b), c) Partial view of diagram a) showing the field structure relatively to the incoming fields A_{01} and A_{02} respectively. d) Diagram of two equal and colinear resonators coupled by a common mirror. The transmitted intensity of the system, given by the expression:

$$\left|\frac{A_T}{A_{IN}}\right|^2 = \left[1 + \frac{[(1+r^2)r_x/2r + \cos(4\pi\nu d/c)]^2}{(1-r^2)(1-r_x)/4r^2}\right]^{-1} \tag{21}$$

The two resonance frequencies $\nu_\pm$ of the system are given by the formula:

$$\nu_\pm = \nu_0 \pm \frac{c}{2\pi d_0} \arctan\left[\frac{2r-(1+r^2)r_x}{2r+(1+r^2)r_x}\right]^{1/2} \tag{22}$$

The formula requires that $r_x \leq 2r/(1+r^2)$. In the case of equality the coupling between the two resonators is minimum and each resonator gets the proper resonance frequency ν_0. If r_x is zero, the coupling is maximum

and it is also maximum the difference between the two resonant modes: $\nu_+ - \nu_- = c/4d_0$.

Fig.6 - Curves of function $S(\nu_g)/\nu_0$ versus the GW frequency of the interferometric antenna in the narrow band case. The function $S(\nu_g)/\nu_0$ is peaked to ν_g^0 frequency and exhibits a ν_g^0/η_E width. The figure shows the tuning of four frequencies of antenna corresponding to the coupling phases $\phi = \pi$, $\pi/3$, $\pi/6$ and $\pi/9$ respectively.

Fig. 7 - Transmitted and reflected intensities of the interferometric antenna optical system versus the parameter $x = \sqrt{2\eta_R}2\Delta\nu/\nu_{FP}$ in the case of GW perturbation.

Fig. 8 - Phase behaviour of symmetric and antisymmetric resonant modes of the optical system in the narrow band version of the interferometric antenna. Phases are plotted versus the phase $\phi = 2ka$ changing the coupling between the two long FP cavities of antenna.

Fig. 9 - Behaviour of parameter t giving the goodness of the approximation $|F|^2 \simeq (1-2t)^2 \simeq 1$ relatively to the conditions $r_1^2 < r_2^2 \simeq \sigma \simeq 1$. The t plot is given versus the cutoff frequency ν_g^0 and two more horizontal scales are added showing the corresponding values of the front mirror reflectivity r_1^2 and the FP finesse F^*.

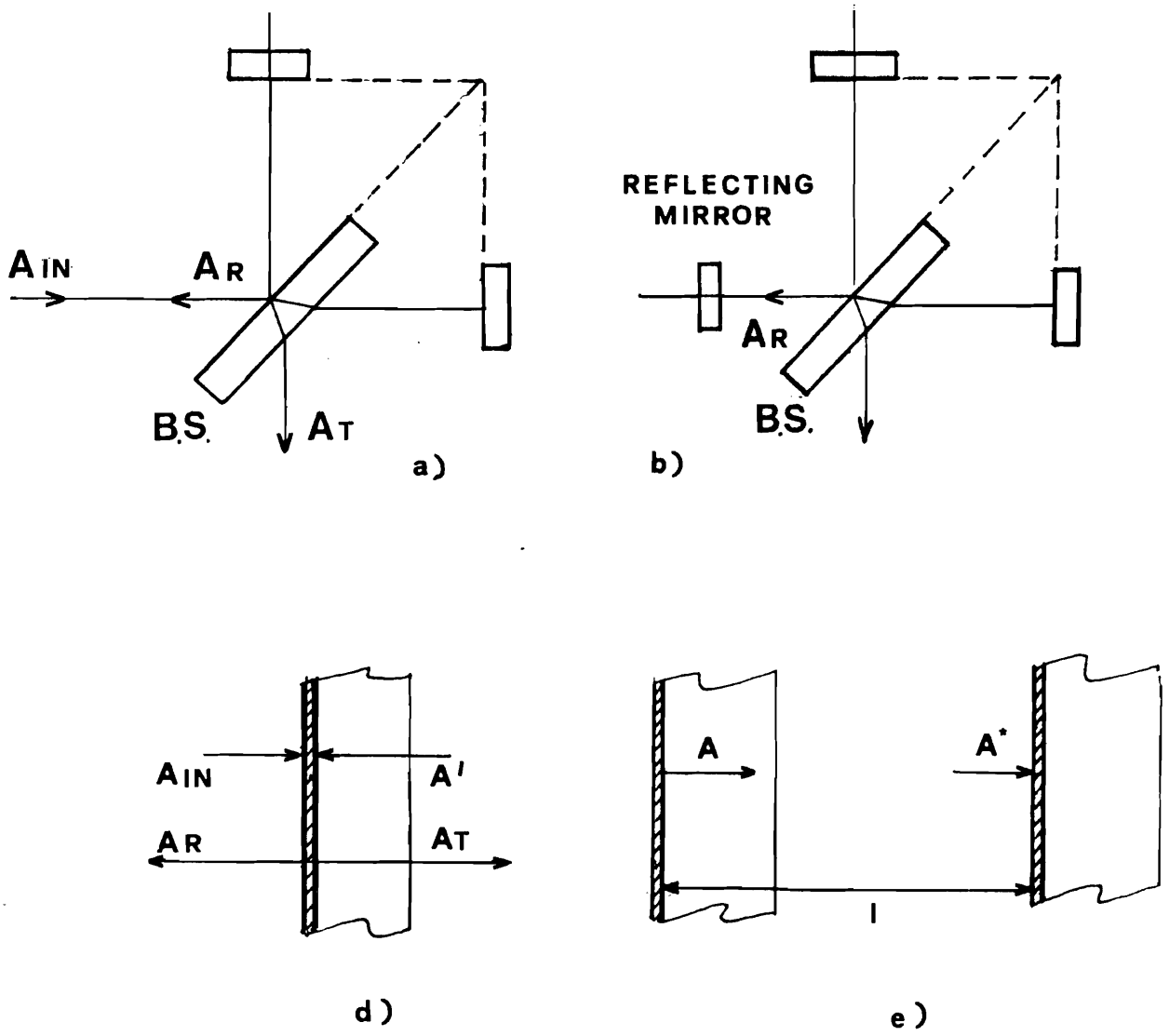

Fig.1

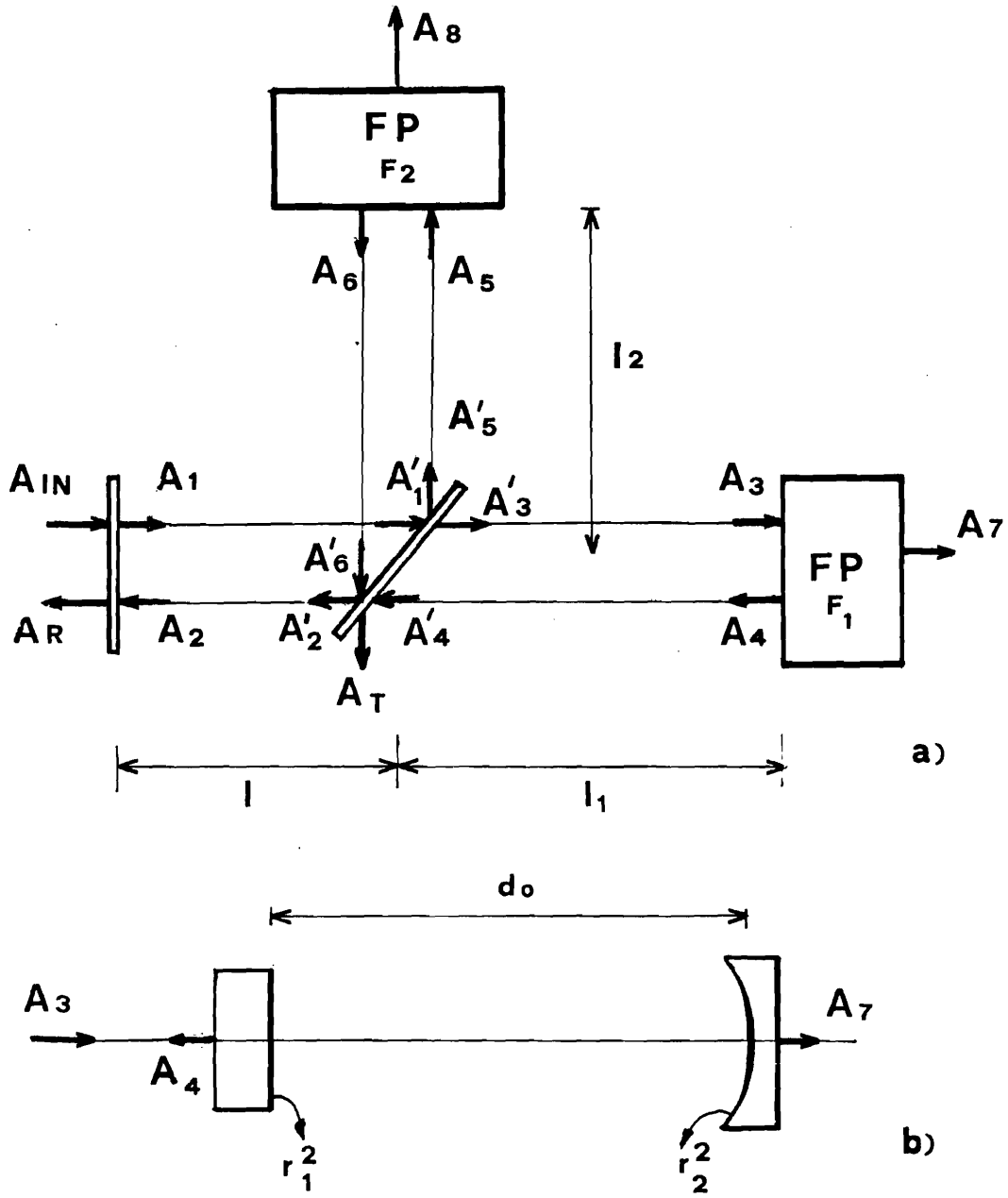

Fabry-Perot resonator

Fig. 2

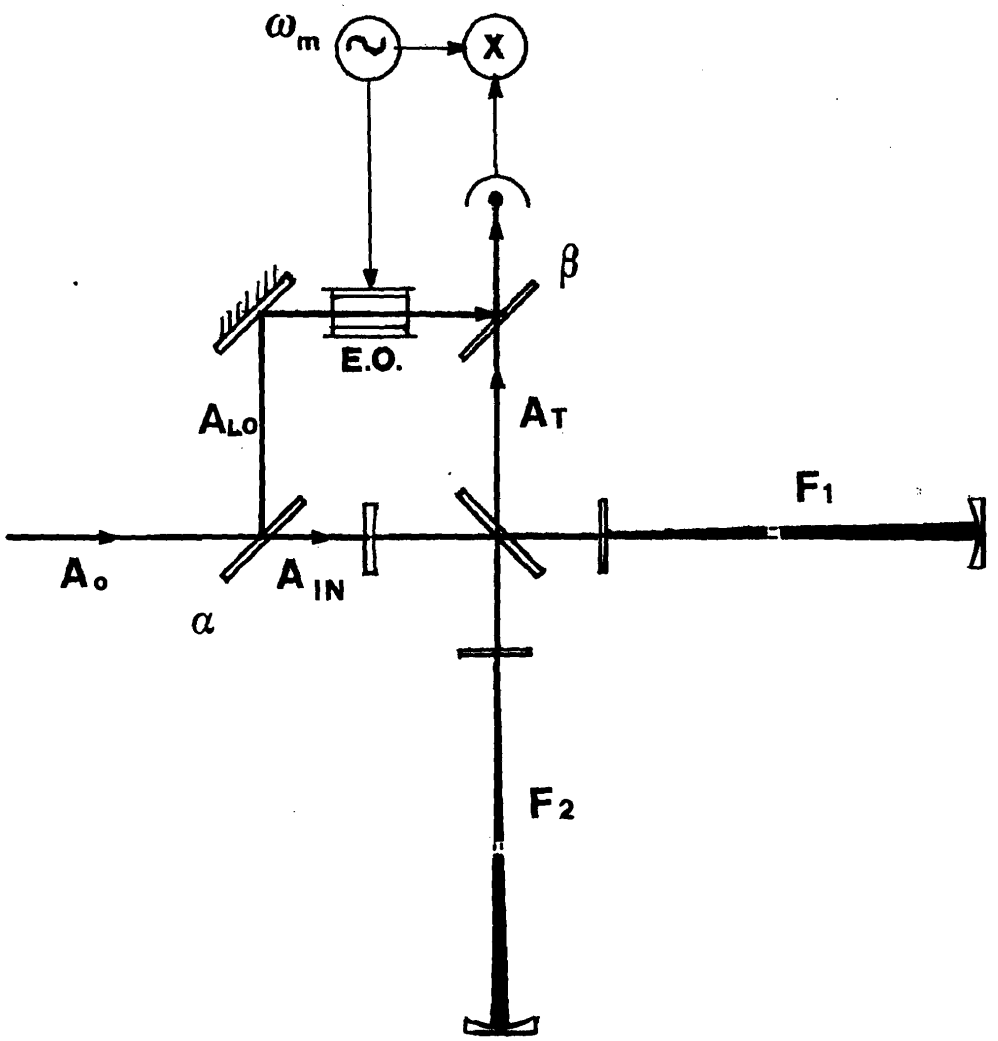

Fig. 3

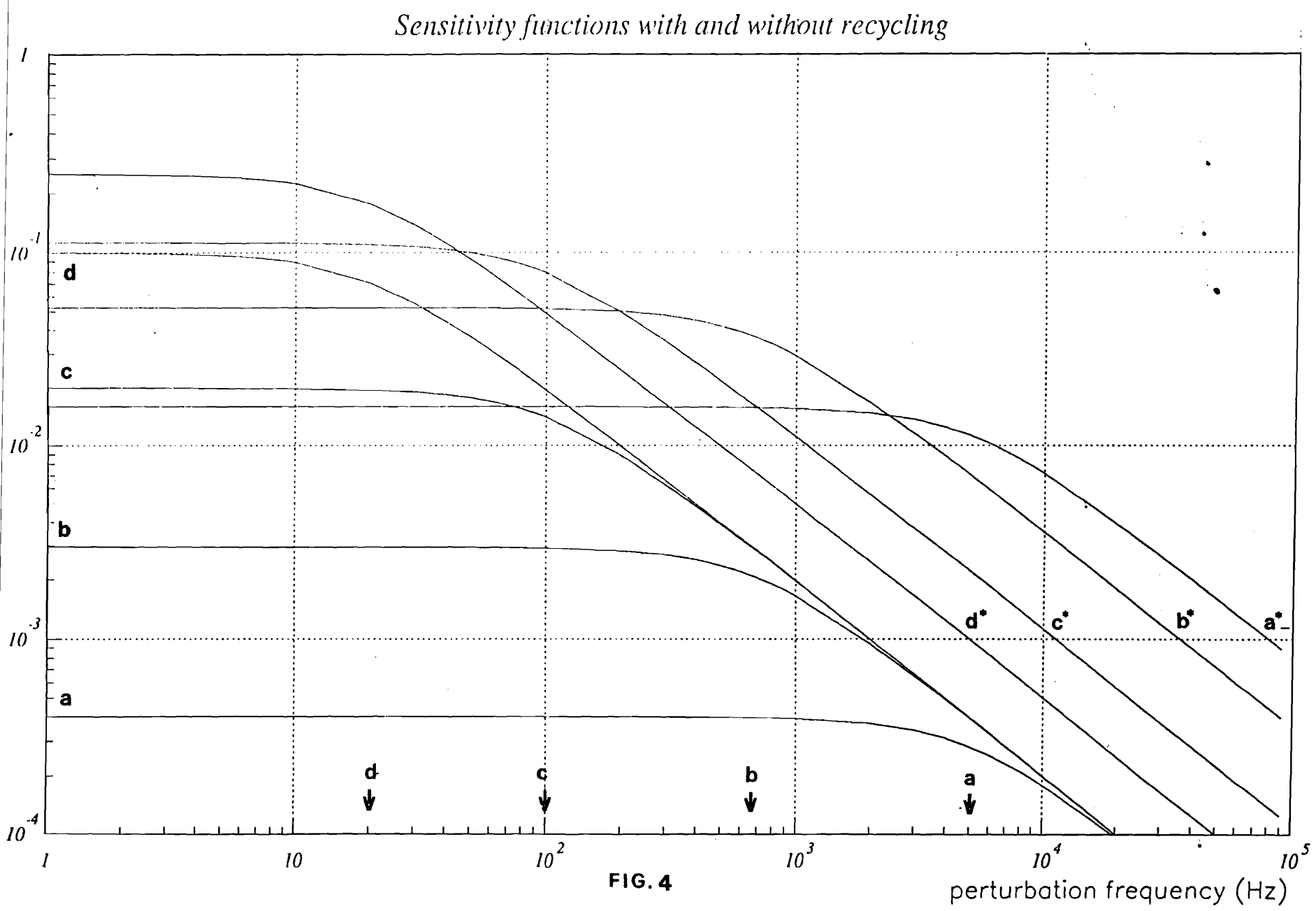
Sensitivity functions with and without recycling
1
10^-1
10^-2
10^-3
10^-4
d
c
b
a
d*
c*
b*
a*
d
c
b
a
1
10
10^2
10^3
10^4
10^5
perturbation frequency (Hz)

FIG. 4

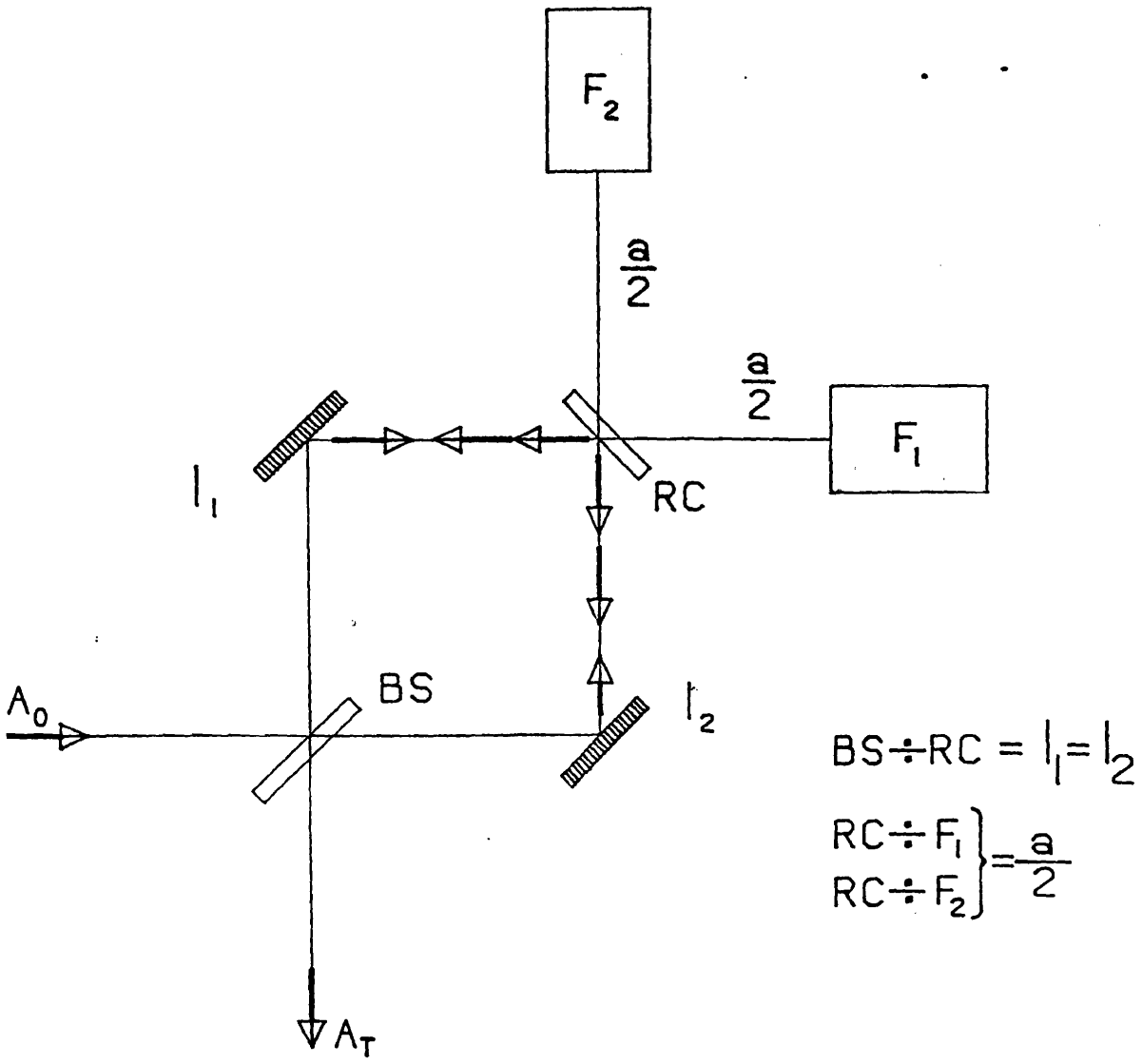

Fig.5a

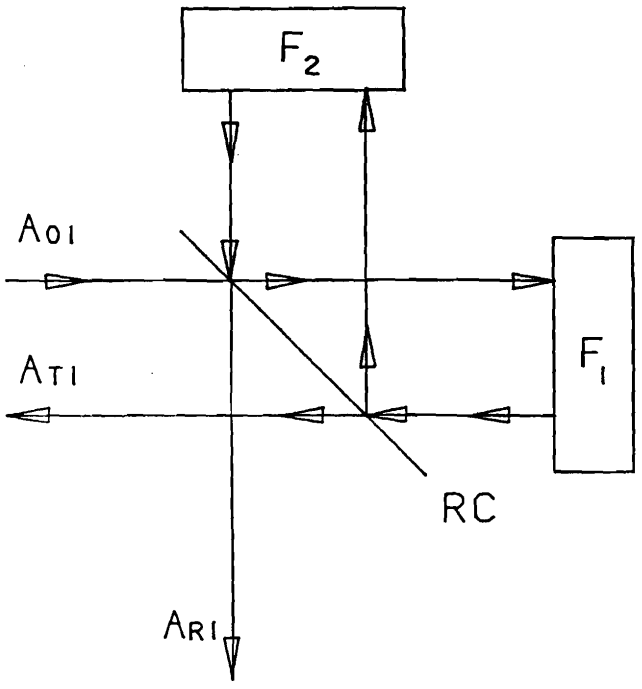

Fig.5,b

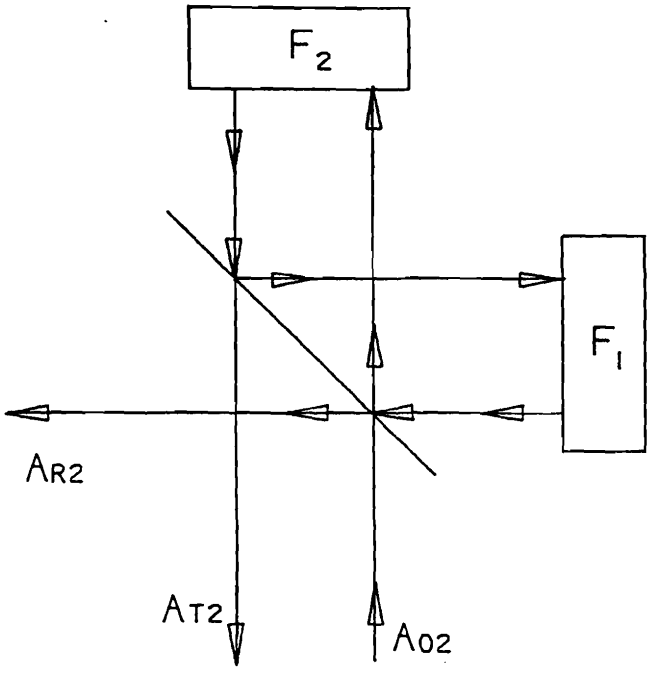

Fig.5,c

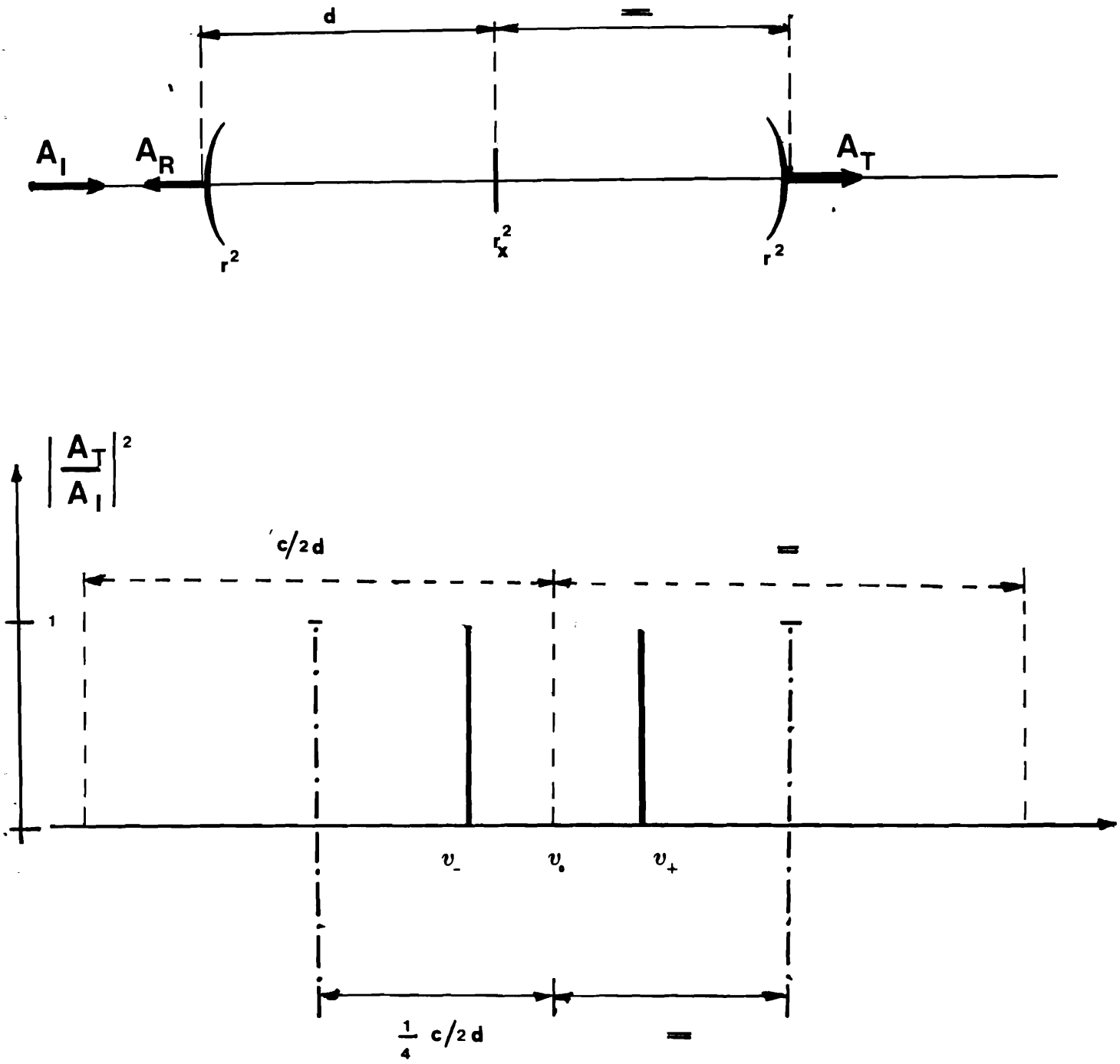

Fig. 5 d)

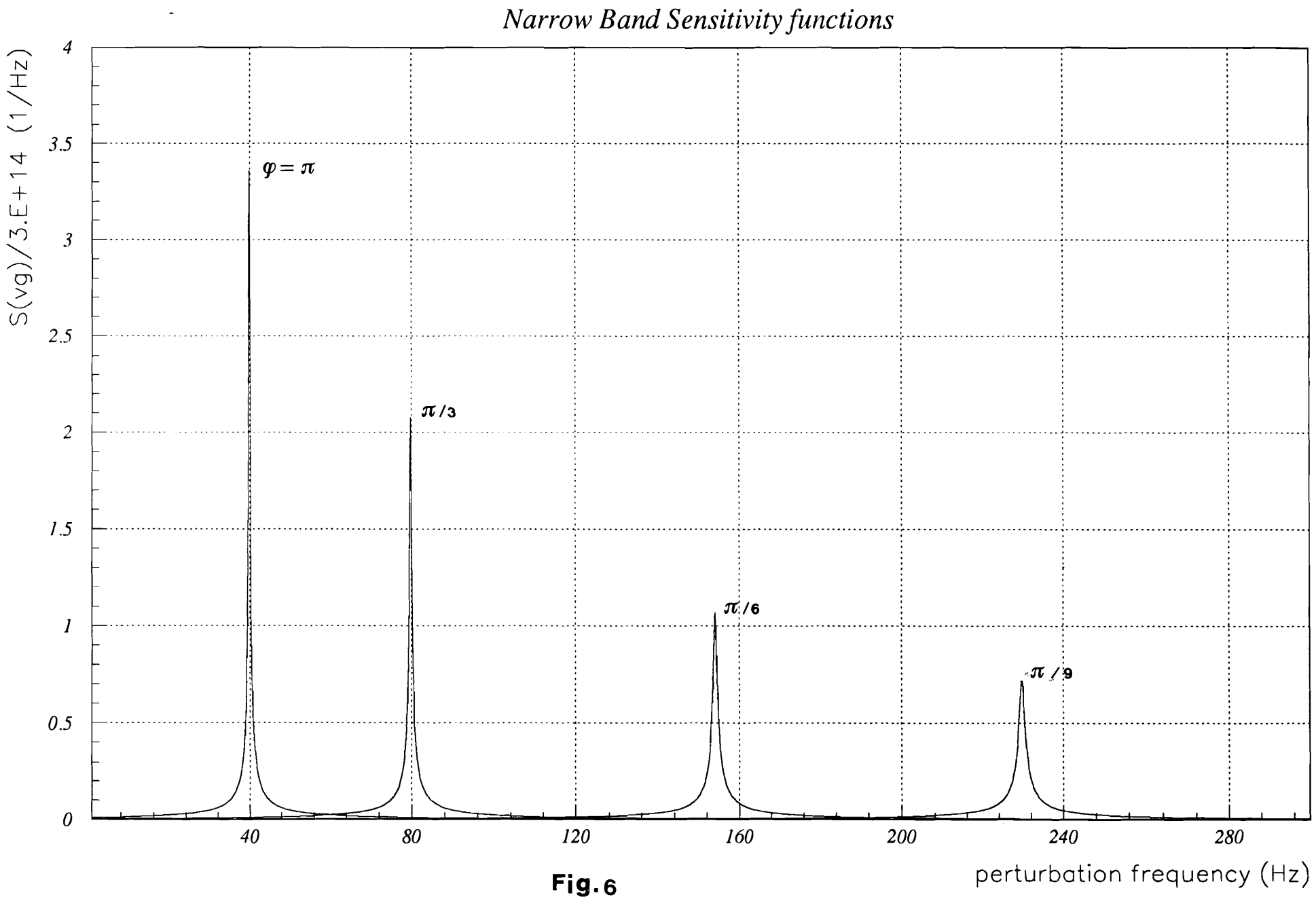
Narrow Band Sensitivity functions
S(vg)/3.E+14 (1/Hz)
4
3.5
3
2.5
2
1.5
1
0.5
0
φ = π
π/3
π/6
π/9
40
80
120
160
200
240
280
perturbation frequency (Hz)

Fig. 6

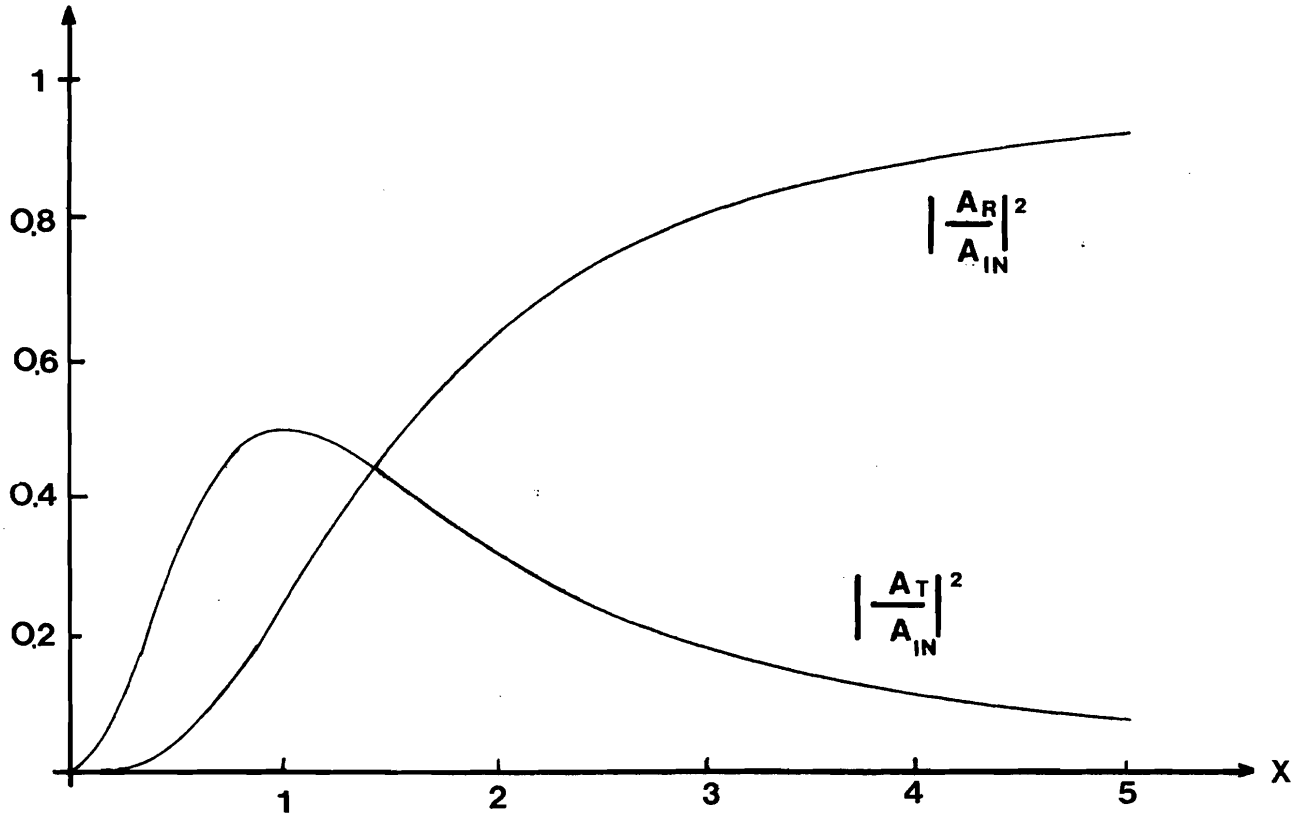
1
0,8
0,6
0,4
0,2
1
2
3
4
5
X
$\left|\frac{A_R}{A_{IN}}\right|^2$
$\left|\frac{A_T}{A_{IN}}\right|^2$

Fig.7

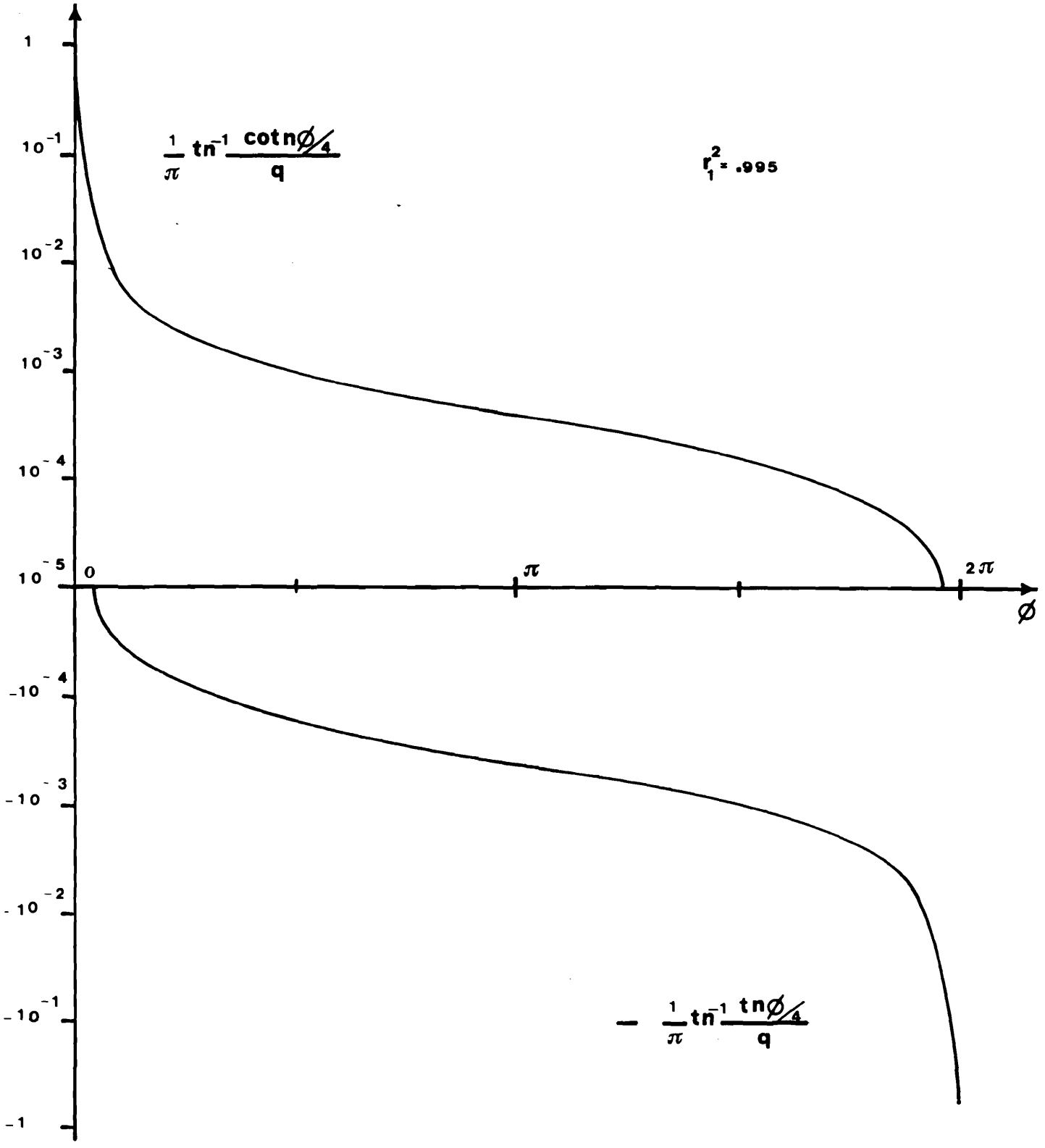
1
10^{-1}
10^{-2}
10^{-3}
10^{-4}
10^{-5}
0
π
2π
ϕ
-10^{-4}
-10^{-3}
-10^{-2}
-10^{-1}
-1
$\frac{1}{\pi}\,\mathrm{tn}^{-1}\,\frac{\mathrm{cotn}\,\phi/4}{q}$
$r_1^2 = .995$
$-\frac{1}{\pi}\,\mathrm{tn}^{-1}\,\frac{\mathrm{tn}\,\phi/4}{q}$

Fig. 8

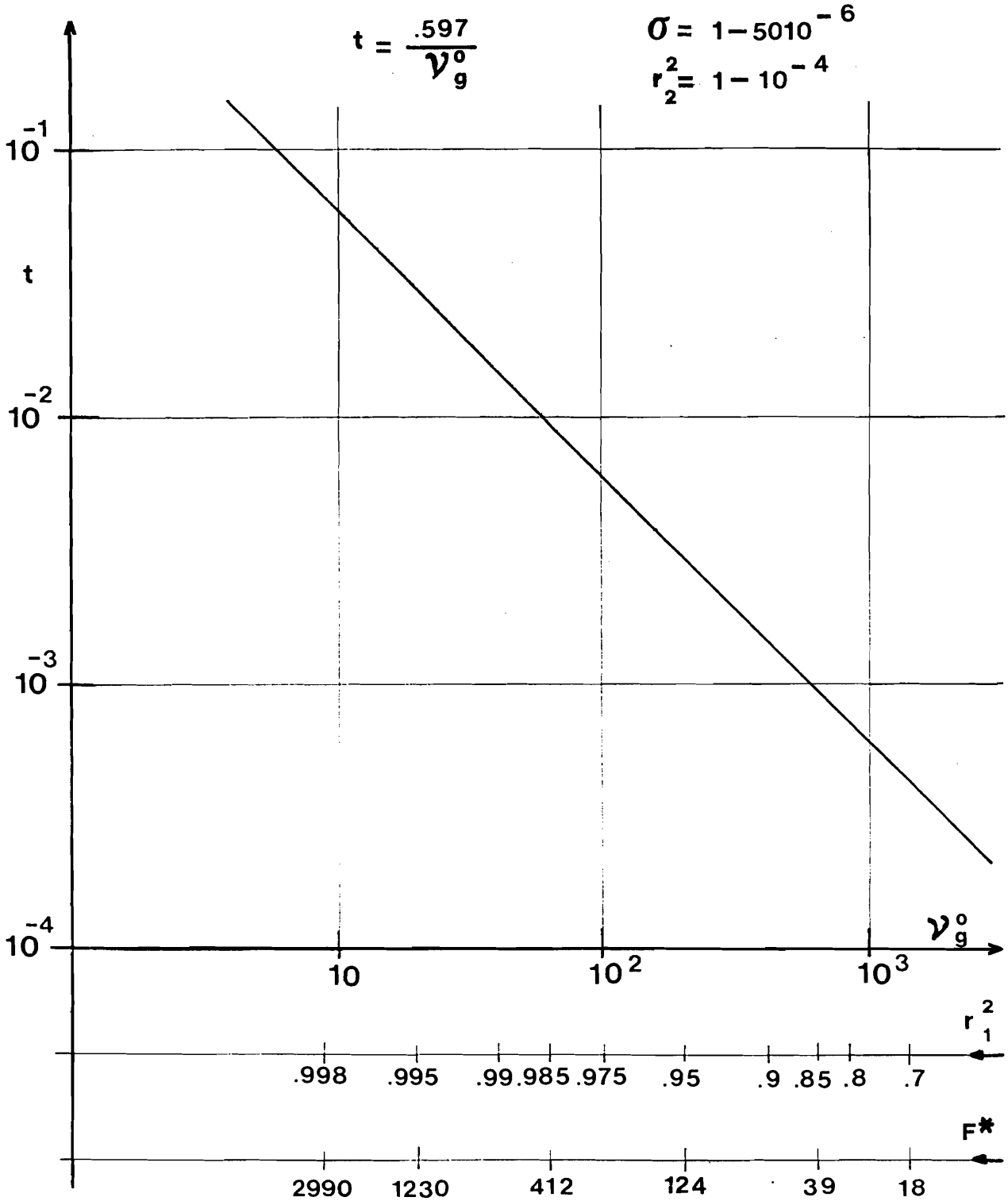
$t = \frac{.597}{\nu_g^o}$
$\sigma = 1 - 5010^{-6}$
$r_2^2 = 1 - 10^{-4}$
10^{-1}
t
10^{-2}
10^{-3}
10^{-4}
ν_g^o
10
10^2
10^3
r_1^2
.998 .995 .99 .985 .975 .95 .9 .85 .8 .7
F^*
2990 1230 412 124 39 18

Fig.9